Andean Geology 50 (3): 403-435. September, 2023
doi: 10.5027/andgeoV50n3-3453

Andean Geology
www.andeangeology.cl

Taphonomic analysis of Spinicaudata from two Triassic lacustrine systems affected by different volcanic processes

***Evelyn Luz Bustos-Escalona[1], Adriana Cecilia Mancuso[1], Cecilia Andrea Benavente[1, 2], Andrea Beatriz Arcucci[3]**

[1] *Instituto Argentino de Nivología, Glaciología y Ciencias Ambientales (IANIGLA), CCT-CONICET-Mendoza, Adrián Ruiz Leal s/n -Parque Gral. San Martín, (5500), Mendoza, Argentina.*
ebustos@mendoza-conicet.gob.ar, amancu@mendoza-conicet.gob.ar, cebenavente@gmail.com
[2] *Geología, Facultad de Ciencias Exactas y Naturales (FCEN), Universidad Nacional de Cuyo (UNCuyo), CP 5500 Mendoza, Argentina.*
[3] *IMIBIO-CONICET, Área de Zoología, Facultad de Química, Bioquímica y Farmacia (FGByF), Universidad Nacional de San Luis (UNSL), Ejército de los Andes 950, (5700), San Luis, Argentina.*
andrea.arccuci@gmail.com

* *Corresponding author: ebustos@mendoza-conicet.gob.ar*

ABSTRACT. Spinicaudata are freshwater branchiopods. The growth and development of spinicaudata populations in freshwater environments depend on various physical, chemical, and biological factors. The action of volcanism modifies the limnological parameters in the process of fossilization of lacustrine deposits. This study identifies spinicaudatan assemblages in two Triassic lake systems in Argentina, and analyzes the dynamics of shell preservation according to the volcanic activity involved. Two taphonomic grades divided into three different second taphonomic grades were defined. The focus on taphonomic and chemistry studies addresses changes in spinicaudata abundance and richness through time, in different paleoenvironmental conditions, and shell preservation and chemical composition. The discussion highlights the importance of lava flow inflow and volcanic ash fall in the different lake systems. We emphasize the importance of taphonomic studies on the spinicaudata groups to understand their autochthonous and allochthonous populations in Triassic lake systems. In turn, we conclude that the *post mortem* processes experienced by the shells, the exposure time at the water-sediment interface, and the chemical alteration of the water into the paleolakes produced by the surrounding volcanic activity can explain the development and preservation of spinicaudata in these two Triassic lacustrine systems.

Keywords: Freshwater branchiopods, Los Rastros Formation, Agua de la Zorra Formation, Triassic, Argentina.

RESUMEN. Análisis tafonómico en Spinicaudata de dos sistemas lacustres triásicos afectados por diferentes procesos volcánicos. Los “espinicaudados” (Spinicaudata) son branquiópodos de agua dulce. El crecimiento y el desarrollo de las poblaciones de “espinicaudados” en entornos de agua dulce dependen de diversos factores físicos, químicos y biológicos. La acción del vulcanismo modifica los parámetros limnológicos en el proceso de fosilización de los depósitos lacustres. Este estudio identifica los ensambles de “espinicaudados” en dos sistemas lacustres del Triásico, en Argentina, y analiza la dinámica de preservación de las conchas según la actividad volcánica involucrada. Se definieron dos grados taxonómicos divididos en tres segundos grados tafonómicos diferentes. El enfoque de los estudios tafonómicos y químicos aborda los cambios en la abundancia y riqueza de los “espinicaudados” a través del tiempo y en diferentes condiciones paleoambientales, así como la preservación y composición química de las conchas. En la discusión se destaca la importancia de la afluencia de lava y de la caída de cenizas volcánicas en los diferentes sistemas lacustres. Enfatizamos la importancia de los estudios tafonómicos sobre los grupos de “espinicaudados” a la hora de proponer la comprensión de sus poblaciones autóctonas y alóctonas de los sistemas lacustres triásicos. A su vez, se concluye que los procesos *post mortem* experimentados por las conchas, el tiempo de exposición en la interfase agua-sedimento y la alteración química del agua en los paleolagos producida por la actividad volcánica circundante pueden explicar el desarrollo y preservación de los spinicaudata en estos dos sistemas lacustres del Triásico.

Palabras clave: Branquiópodos de agua dulce, Formación Los Rastros, Formación Agua de la Zorra, Triásico, Argentina.

1. Introduction

Spinicaudata are small branchiopods that inhabit small, shallow, temporary ponds, being typically found in the coastal and photic zone of lakes and lagoons (*e.g*., Tasch, 1969; Webb, 1979). Spinicaudata can be considered r-strategist species because they produce resistant eggs. The growth and development of spinicaudata populations in these environments depend on physical, chemical, and biological factors. However, they have a high tolerance to variations in environmental conditions during the growth phase, such as temperature (from 1 to 41°C), oxygenation, pH (from 7 to 9.7), and salinity (from 6 to 35), which facilitates the development of populations in different environments (Gislén, 1937; Massal, 1954; Rzoska, 1961; Tasch and Zimmerman, 1961; Bishop, 1967; Horne, 1967; Moore and Burn, 1968; Kobayashi, 1975; Webb, 1979; Tasch, 1987; Gore, 1988; Fryer, 1996; Thiéry, 1996; Cáceres and Tessier, 2003; Ferreira Olivera, 2007; Benvenuto *et al*., 2009; Astrop *et al*., 2012; Tassi, 2015). The co-occurrence of two or more species in the same environment is favored by morphologic and phylogenetic differences among them (Orr and Briggs, 1999; Dumont and Negrea, 2002), being more frequently monospecific communities (Spencer and Hall, 1896; Tasch and Shaffer, 1964; Moore, 1965; Tasch, 1969; Ferreira-Olivera, 2007; Astrop *et al*., 2012; Tassi, 2015). The nutrient availability, such as the variety and quantity of algae, microplankton, and bacteria, is one of the biological limiting factors for developing a diverse spinicaudata population (Kapler, 1960; Petr, 1968; Royan, 1976).

Taphonomic studies on spinicaudata are mainly based on mechanical features (Krishnan, 1958; Rieder *et al*., 1984; Zhang *et al*., 1990; Orr *et al*., 2002, 2008; Olempska, 2004; Mancuso and Marsicano, 2008; Astrop and Hegna, 2015; Astrop *et al*., 2015; Bustos Escalona *et al*., 2017; Jenisch *et al*., 2017), or chemical composition of post-buried shells (Briggs, 2003; Stigall *et al*., 2008; Astrop and Hegna, 2015; Astrop *et al*., 2015; Monferran *et al*., 2018; Hu *et al*., 2020). The spinicaudata shell is mainly composed of a calcium-phosphate complex (*e.g*., Astrop *et al*., 2015), and the multi-laminar structure of shells makes it resistant to taphonomic processes such as decay, desiccation, and compaction (Krishnan, 1958). Astrop and Hegna (2015) suggest that the mechanical features of spinicaudata shells are specific to taxonomic families. Moreover, the chemical composition of the shell generates differences in the fossilization process, also favoring the prevalence of some taxa in the fossil record (Briggs, 2003; Astrop and Hegna, 2015; Astrop *et al*., 2015; Hegna *et al*., 2020). However, Astrop *et al*. (2015) conclude that despite variation in cuticle chemistry, the degree of mineralization alone does not predict the mechanical properties of shells and that post-depositional taphonomic processes such as permineralization and dissolution also need to be analyzed.

Post mortem modifications reflect the alterations suffered by the remains, including cracking, surface marks, abrasion, polishing, and fracture (*e.g*., Behrensmeyer and Hook, 1992; Behrensmeyer *et al*., 2000; Mancuso and Marsicano, 2008; Astrop *et al*., 2015; Karr and Clapham, 2015). Each type of these modifications indicates a taphonomic process and may be diagnostic of a specific agent. Mechanical abrasion on carbonate skeletons can occur either as a result of repeated reworking within a high-energy environment or during long-distance transport (*e.g*., Behrensmeyer and Hook, 1992; Behrensmeyer and Kidwell, 1985; Behrensmeyer *et al*., 2000; Mancuso and Marsicano, 2008; Astrop *et al*., 2015; Karr and Clapham, 2015), as observed on marine mollusk shells (Behrensmeyer *et al*., 2000; Brett and Baird, 1986; Behrensmeyer and Hook, 1992). Bioerosion has also been recorded in carbonate rocks from marine environments (Golubic and Schneider, 1979) and spinicaudatan shells from lacustrine paleoenvironments (Bustos Escalona *et al*., 2019). The abrasion, combined with a long time at the sediment-water interface before burial, promotes the dissolution of the carbonate shells (Brett and Baird, 1986). Likewise, dissolution is a taphonomic alteration that is highly selective in terms of chemical and mineralogical composition, size, and microstructure of the fossil particles or fragments. The resistance of the elements to dissolution is related to the stability of their mineral components, effective surface area, and other factors such as their microstructure and permeability (*e.g*., Plotnick, 1986; Wilson, 1988; Behrensmeyer, 1991; Behrensmeyer and Hook, 1992; Behrensmeyer *et al*., 2000; Astrop *et al*., 2015; Karr and Clapham, 2015). Most of the shell spinicaudatan fossils, which were chemically analyzed, have been preserved as recrystallized calcium phosphate or silica replaced molds (Stigall and Hartman, 2008; Stigall *et al*., 2008, 2014; Hethke *et al*., 2013; Monferran *et al*., 2018; Hu *et al*., 2020).

In tectonically active areas, the record of volcanic material and sediment is widespread. Volcanoes produce large amounts of loose sediments that affect local deposit systems, destroy surrounding biotic habitats, change river flows, transform topography, and cause changes in the physical and chemical conditions of sedimentary environments (Lipman and Mullineaux, 1982; Smith, 1987; Lockley and Rice, 1990; Behrensmeyer and Hook, 1992; Dale *et al*., 2005; Payne and Egan, 2017). The volcanic eruption impact depends on the explosion magnitude and varies according to the distance from the center of the volcanic activity (Payne and Egan, 2017). Particularly in lacustrine systems, the volcanic activity increases the rate of sediment supply by the unusual ash fall and lava flow supply, which also triggers changes in the original chemical composition of lake waters and microenvironmental diagenetic conditions (Behrensmeyer and Hook, 1992). The lava flows cause alteration of the limnological parameters, both physical (*e.g*., temperature and habitat reduction) and chemical (*e.g*., pH and salinity). The entry of volcanic ash into aquatic ecosystems also produces alterations in limnological parameters (*e.g*., increase in turbidity, changes in pH, conductivity, variations in nutrient concentration), which directly affect the surrounding biota from a basal trophic level (*e.g*., decrease in primary productivity due to modification of the microbial community) and thus modify the trophic state (Barker *et al*., 2000; Okorafor, 2011; Massaferro *et al*., 2018; Pedernera *et al*., 2021). Despite the evident adverse effects of volcanic activity on the surrounding ecosystems, the fossil record in lake deposits could be favored by the action of volcanism (Beherensmeyer and Hook, 1992; Pan *et al*., 2011).

This work therefore aims to identify the taphonomic processes that affect the spinicaudata fossil assemblages found in two Triassic lacustrine systems, in Argentina, and investigates how the spinicaudata shells preservation was affected by volcanic activity (*i.e*., ash fall and basaltic lava flows) in the Triassic lacustrine environments.

2. Geological setting

Triassic sedimentation in Argentina occurred in extensional basins associated with the breakup of Pangea, which began in the latest Permian-earliest Triassic (Uliana and Biddle, 1988; Lovecchio *et al*., 2020). Two of the largest basins were developed along the southwestern margin of Gondwana (Fig. 1), with NNW-SSE trends related to basement fabric control (Martínez *et al*., 2011). The basins were filled by thick, entirely continental successions of predominantly fluvial and lacustrine sediments that record almost the whole Triassic.

In the Ischigualasto-Villa Unión Basin (San Juan and La Rioja provinces) (Fig. 1A), the Los Rastros Formation (LRF) represents a lacustrine-deltaic succession characterized by shallowing-upwards cyclic deposits of dark gray to black mudstone, siltstone, and tabular fine to coarse-grained sandstone. At the Gualo locality (Talampaya National Park, La Rioja province) (Fig. 1B-C), the outcrops are characterized by five lacustrine-deltaic cycles (Fig. 2A). Each cycle is characterized by horizontally laminated gray-black claystone (Fl) occasionally interbedded with iron mudstone (SFm), which represents the distal lacustrine and prodelta deposits (LR-A facies association-Table 1). The distal lacustrine and prodelta sediments pass upward to mudstone (Fm) and fine to coarse-grained sandstone (Sr, Sh, Sp, St, SG) deposited by progradation of a mouth-bar complex in an upward-shallowing delta front environment (LR-B facies association-Table 1). Then, medium- to coarse-grained sandstone interbedded occasionally with coal mudstone (FCS) is deposited by a distributary fluvial system with delta swamps on a deltaic plain (LR-C facies association-Table 1) (Mancuso and Marsicano, 2008; Mancuso and Caselli, 2012; Mancuso *et al*., 2020). The LRF records a syn-rift phase in the Ischigualasto-Villa Unión rift Basin (Mancuso and Caselli, 2012; Mancuso *et al*., 2020). The stratigraphic relation with the isotopically dated Chañares and Ischigualasto formations and the recent CA (Chemical Abrasion)-TIMS analysis of a tuff level from the LRF at Cerro Bola locality (234.47±0.44 Ma), suggest that LRF covers a significant part of the Carnian (Mancuso *et al*., 2020).

The Cuyana Basin (Mendoza, San Juan, and San Luis provinces), includes the Agua de la Zorra Formation (AZF), exposed at the Paramillos de Uspallata locality (Fig. 1D-E), is interpreted as deposited in a lacustrine-deltaic setting with episodic incursions of lava flows into the aquatic environment (Ottone *et al*., 2011; Pedernera *et al*., 2019). The succession is characterized by mudstone (Fm) interbedded with fine to coarse-grained sandstone (Sm, Sr, St) deposited by progradational deltas with development of mouth bars (AZ-A facies association-Table 2).

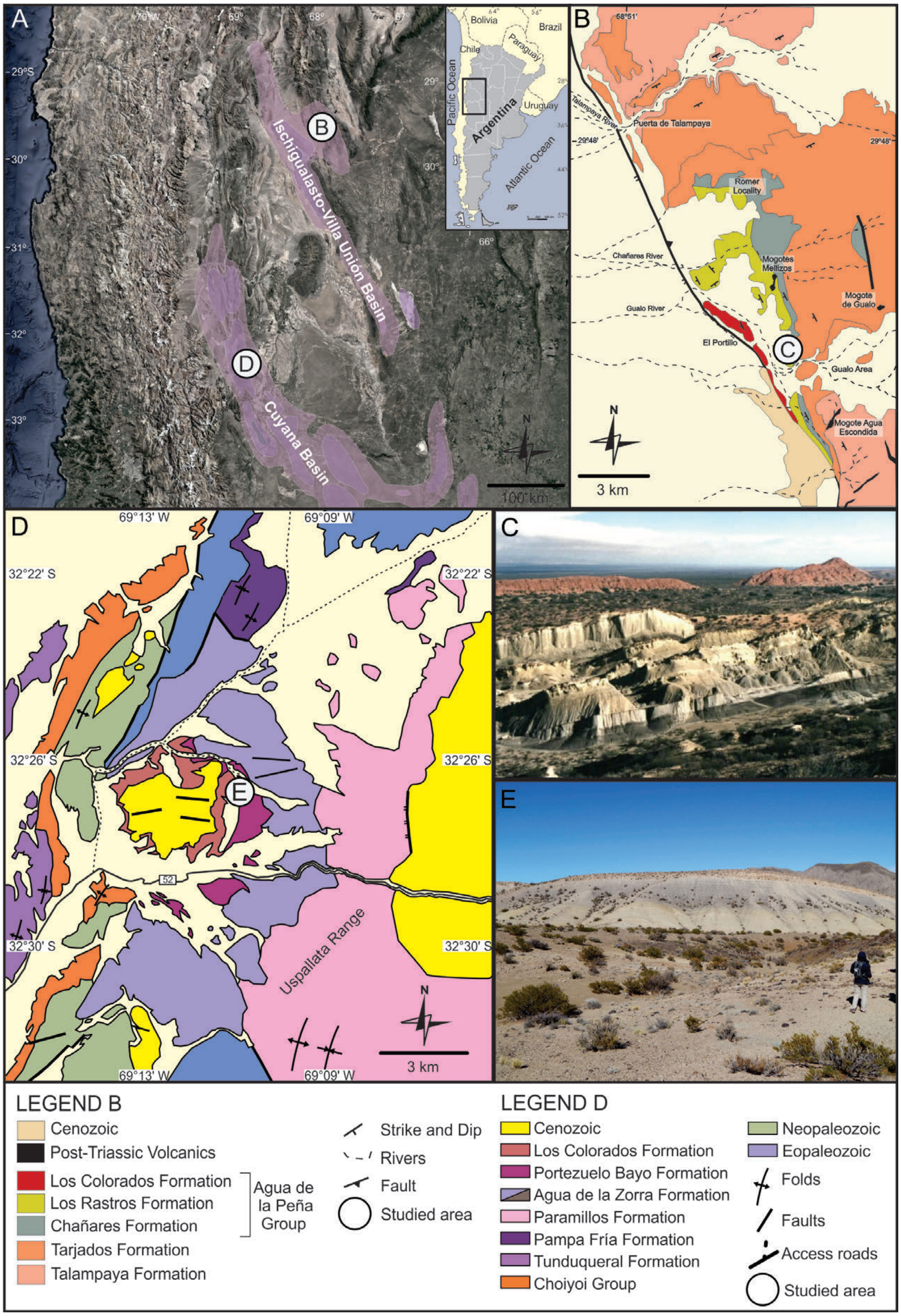

FIG. 1. Geographical location of the Ischigualasto-Villa Unión and Cuyana Basins, central-western Argentina. **A.** Satellite image of the study area (Inset: regional context). **B.** Geological map of the Gualo-Chañares area in the Talampaya National Park, Ischigualasto-Villa Unión Basin. **C.** Panoramic photograph of the Los Rastros Formation outcrop (see photo location in B). **D.** Geological map of the Paramillos de Uspallata area, Cuyana Basin. **E.** Panoramic photograph of the outcrop of Agua de la Zorra Formation (see photo location in D).

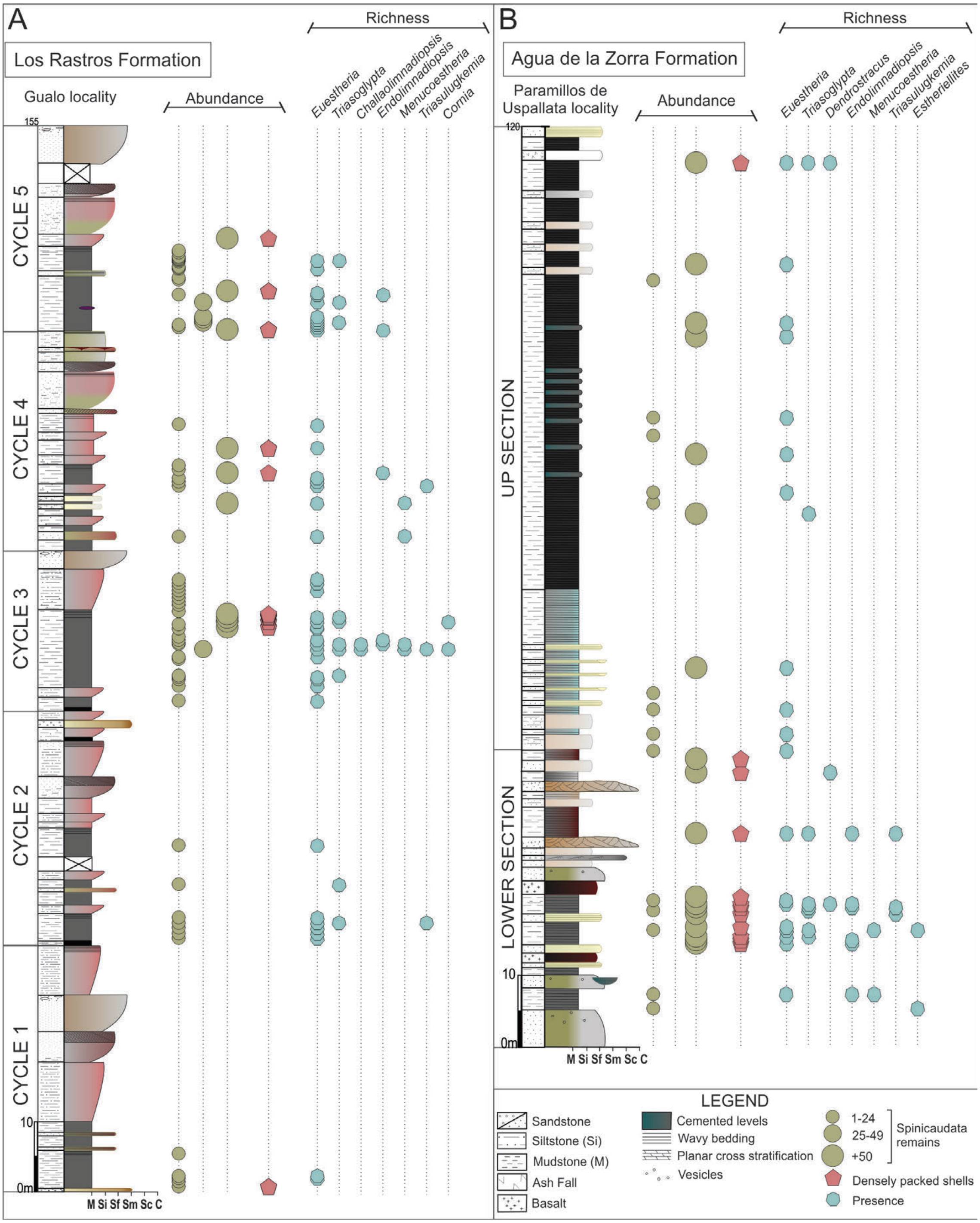

FIG. 2. Record of the abundance, richness, and stratigraphic distribution of the spinicaudata remains for **A.** The Los Rastros Formation. **B.** The Agua de la Zorra Formation. **M:** Mudstone, **Si:** Siltstone, **Sf:** Fine-grained Sandstone, **Sm:** Medium-grained Sandstone, **Sc:** Coarse-grained Sandstone, **C:** Conglomerate.

TABLE 1. FACIES ASSOCIATIONS AND THEIR CHARACTERISTICS DEFINED FOR THE LOS RASTROS FORMATION, ISCHIGUALASTO-VILLA UNIÓN BASIN, TALAMPAYA NATIONAL PARK, LA RIOJA PROVINCE.

Facies Association (FA) and Interpretation	Facies	Sedimentary structures	Bed geometry	Fossil Content	Vertical and lateral relations
LR-A Distal lacustrine and prodelta	Claystone and fine-grained siltstone **(Fl)**	Thinly horizontally laminated, locally fissile or massive gark gray and black carbonaceous	Tabular, 0.4-2 m thick. Individual massive beds are 1-5 cm in thickness	Palynomorph and algae, plant, insect, spinicaudata and fish remains	Overlies facies Fl, Wm, Sl, Fm, Sh, Sp, St
	Mudstone and fine-grained sandstone **(SFm)**	Massive, horizontally laminated, very dusky purple, and rarely silty and sandy beds normally graded	Tabular, 0.01-0.3 m thick. Abrupt upper and lower contacts, exhibiting rare erosive bases	Plant, spinicaudata, fish, and sporadically fish locomotion traces	SFm facies is interbedded with Fl facies, and pass laterally to Fl facies
LR-B Deltaic front with progradation of the mouth bar	Siltstones and claystone **(Fm)**	Gray Massive siltstone and claystone alternate on a cm-scale	Tabular, 5-20 m thick. Individual beds are tabular and 0.1 m thick with non-erosional boundaries	Plant and spinicadata	Fm facies overlies Fl facies
	Ripple cross-lamination, horizontal lamination sandstones **(Sr, Sh)**	Moderate to well sorted fine- to medium-grained sandstone ripple cross-lamination, horizontal lamination, small-scale hummocky cross-stratification grayish orange	Tabular to planar-convex, 0.05-0.6 m thick	Plant, fish, spinicaudata, and rare invertebrate traces	Facies overlie Sr, Sh, Sp, St
	Horizontal lamination, planar to trough cross-stratification sandstones **(Sh, Sp, St, SG)**	Moderate to well sorted medium- to coarse-grained sandstones, rare sandy conglomerate, grayish orange to grayish olive horizontal lamination, planar to trough cross-stratification	Tabular to plane-convex, 0.5-3 m thick	Plant and rare invertebrate traces	Facies overlie Sh, Sp, St
LR-C Delta plain with distributary fluvial system and delta swamps within the delta plain	Planar to trough cross-stratification sandstones **(Sp, St)**	Moderate to well sorted medium- to coarse-grained sandstones, planar to trough cross-stratification grayish orange and yellowish gray, locally ripple cross-lamination at the top of beds	Lenses to tabular, 0.1-3 m thick. Erosional basal boundaries and planar upper boundaries. Co-sets are 0.3-0.6 m in thickness	Plants, and invertebrate traces	Facies overlie Sp, St
	Sandstone and coal layers **(FCS)**	Black, dusky brown mudstone to very fine-grained sandstone and coal layers, massive, horizontal lamination, and ripple cross-lamination	Tabular, 0.2-0.5 m thick	Carbonized plant and plant debris	FCS facies is interbedded with Sp, St facies

Taken and modified from Mancuso and Caselli, 2012.

TABLE 2. FACIES ASSOCIATIONS AND THEIR CHARACTERISTICS DEFINED FOR THE AGUA DE LA ZORRA FORMATION, CUYANA BASIN, PARAMILLOS DE USPALLATA, MENDOZA PROVINCE.

Facies Association (FA) and Interpretation	Facies	Sedimentary structures	Bed geometry	Fossil content	Vertical and lateral relations
AZ-A Delta associated with mouth bars at the delta front	Cemented massive sandstones **(Sm)**	Fine-grained, well-sorted massive sandstones of dark greenish gray color (5GY4/1), with vesicles of 0.5 cm in diameter, carbonate cement interdigitations and carbonate cemented nodules	Tabular, 1-14 m thick	-	Underlies and overlies facies Fl
	Massive siltstones **(Fm)**	Massive muddy siltstones, color is light brownish gray (5YR6/1)	Tabular, 0.3-0.6 m thick	Trace fossils	Overlies facies Sm, Sr, Fl and underlies facies Sr, St, Fl
	Ripple cross sandstones **(Sr)**	Coarse-grained, well sorted sandstones, 1 cm thick sets and 2 cm thick cosets, siliciclasts are subrounded to subangular, containing angular quartz, K-feldspar and muscovite, color is moderate light gray (N6)	Tabular, 0.3 m thick	-	Underlies and overlies facies Fm
	Trough cross sandstones **(St)**	Pebbly sandstones with through cross stratification, sets are 5 cm thick in cosets of 20 cm thick, coarsening upwards	Tabular, 2 m thick	-	Underlies facies Fl and overlies facies St
AZ-B Prodelta to distal lacustrine	Finely laminated mudstones **(Fl)**	Finely laminated mudstones, laminae are 1 mm thick, color range from black (N1) to olive black (5Y2/1) to greenish red (5R4/2) to greenish black (5YR2/1)	Tabular, 0.5-11 m thick	Plant remains, fish scales and spinicaudata	Overlies facies Sm, Sh, St, Fm, Tf
	Massive siltstones **(Fm)**	Massive muddy siltstones, color is light brownish gray (5YR6/1)	Tabular, 0.3-0.6 m thick	Trace fossils	Overlies facies Sm, Sr, Fl and underlies facies Sr, St, Fl
	Horizontally laminated sandstone **(Sh)**	Fine to coarse-grained well sorted-sandstone, lamination is 0.5 cm thick	Tabular to lenticular, 0.3-0.6 m thick	-	Underlies and overlies facies Fl
	Tuff **(Tf)**	Massive, white color (N9)	Tabular, 0.5 m thick	-	Underlies and overlies facies Fm

Up section, black, olive black, greenish-red, and greenish-black mudstone (Fl), occasionally interbedded with muddy siltstone (Fm) and fine to coarse-grained sandstone (Sh), were deposited in a distal lacustrine and prodelta setting (AZ-B facies association-Table 2). The lower section dominated by deltaic deposits is characterized by interlayers of peperitic, olivine basalts interpreted as episodes of lava flow incursions into the aqueous environment (Fig. 2B) (Harrington, 1971; Brea and Artabe, 1999; Ottone *et al*., 2011; Pedernera *et al*., 2019). Deposits of the AZF took place in a continental rift tectonic environment, particularly associated with the syn-rift phase in the evolution of the Cuyana rift Basin (Kokogian and Boggetti, 1987; Uliana and Biddle, 1988; Kokogian and Mansilla, 1989; Ramos and Kay, 1991). Isotopic dating of the basalts of the AZF suggests that the unit was deposited in the Middle-Upper Triassic (240±10 to 235±5 Ma)

(Massabie *et al*., 1986; Ramos and Kay, 1991; Linares, 2007).

Volcanic activity was already recognized in previous stratigraphic studies of both units (Mancuso and Caselli, 2012; Pedernera *et al*., 2019). In the LRF, several tuffaceous levels were interpreted as ash fall and reworked tuff deposits (Mancuso and Caselli, 2012). While, in the AZF, basalt lava flows were identified, including mudstone with peperitic basalt alteration, tuffaceous sandstone, thermally altered sandstone (in the lower section), and ash fall layers interbedded with distal lacustrine facies (in the upper section) (Pedernera *et al*., 2019). Based on the volcanic deposits, the Los Rastros paleolake was located more than 100 km away from the volcanic center (Pedernera, 2020), while the Agua de la Zorra paleolake was developed in the volcano vicinity, approximately within the first 10 km from the eruption zone (Pedernera, 2020).

3. Material and methods

Systematic sampling was carried out every 20 cm throughout the stratigraphic columns corresponding to the Los Rastros (Gualo locality) and Agua de la Zorra (Paramillos de Uspallata locality) formations (Fig. 2). A total of 3,149 spinicaudata remains (1,500 from the LRF and 1,649 from the AZF) were collected mainly from horizontally laminated mudstone (Fl) and mudstone and fine-grained sandstone (SFm) of the distal lacustrine facies association, and in less quantity from siltstone and fine-grained sandstone (Fm/Sh) of the distal delta front facies association. The remains were found predominantly disarticulated, preserving only one of the two shells that constituted the live spinicaudata body. They were positioned on the sediment surface according to their most stable equilibrium state, leaving the external face of the shell up. This position is called the convex-up position in this contribution. The shells are found concordant to the top of the bearing bed, without preferential orientation. A few remains were observed with articulated shells. In this case, the specimens were deposited on the top of the bearing bed with the shells open according to their most stable equilibrium position and also, leaving the external faces of the shell up. In general, the spinicaudata remains were found as compression or shell impressions.

3.1. Taphonomic analyses

The collected samples were characterized into (1) Isolated shells, or (2) Densely Packed shells. The first category comprises rock samples with one or more spinicaudata remains, which could be seen individually, without overlapping each other. The second category includes densely packed shells in mudrocks without condensed time features preserving massive amounts of spinicaudata remains, overlapping each other, and with similar preservation features that discard time-averaging.

All spinicaudata remains were evaluated using a standard semi-quantitative method of scoring preservation quality. The method allows us to define taphonomic grades (TG) to express preservation quality by evaluating the integrity and articulation of fossils. This method has been widely used in the taphonomic analysis of insect and vertebrate assemblages (*e.g*., Wedmann, 1998; Smith and Moe-Hoffman, 2007; McNamara *et al*., 2011, 2012; Wang *et al*., 2013).

A first classification was made according to the fragmentation presented by the spinicaudata shells, resulting in two main TGs: (1) entire shell, and (2) fragmented shell (Table 3). Accordingly, in previous studies, the TGs would indicate the procedence of the spinicaudata shells and their transport time (Fürsich *et al*., 2016; Jenisch *et al*., 2017). In a second-level division, each TG was divided into three different second taphonomic grades (STG) according to the integrity of the morphological characters retained in the shells (STG-*a*, STG-*b*, and STG-*c*) (Table 3). Each STG indicates a progressive loss of definition in the morphological characters such as edges, growth lines, and ornamentation (Table 3). These STGs can thus indicate the time period that the spinicaudata shells laid on the water-sediment surface before burial (Fürsich and Pan, 2015; Hu *et al*., 2020).

3.2. Chemical analyses

The elemental compositions of 52 LRF samples and 19 AZF samples were analyzed by using a JEOL JSM-6610 LV scanning electron microscope (SEM), equipped with an energy dispersive spectrometer (Thermo Scientific Ultra Dry Noran System 7) at the MEBYM Lab, IANIGLA-CONICET. All samples were carbon-coated. We used a live acquisition time of 30 s, nominal incident beam energy E=15 keV,

TABLE 3. DETAIL OF THE CHARACTERS USED IN THE DESIGNATION OF THE VARIOUS TAPHONOMIC GRADES FOR SPINICAUDATA SHELLS OF THE LOS RASTROS FORMATION, ISCHIGUALASTO-VILLA UNIÓN BASIN (CARNIANO, UPPER TRIASSIC) AND AGUA DE LA ZORRA FORMATION, CUYANA BASIN (MIDDLE-UPPER TRIASSIC).

Taphonomic grade	Preservation description	Second level taphonomic grade	Preservation description
1	Entire shell	*a*	It presents both the edges and the well-defined growth lines. The ornamentation in the growth bands is observed
2	Fragmented shell	*b*	It presents defined edges and growth lines between a range of 40% and 70%. Ornamentation is diffuse in the growth bands
		c	The edges and growth lines are diffuse, and no ornamentation is observed in the growth bands

and 10 mm working distance. The results are semi-quantitative. Scanmaps (EDS) were performed from the shell and at the shell-rock matrix interface. The weight percentage of 13 major elements (C, O, F, Al, Si, P, K, Ca, Mn, Mg, Fe, Na, S) was determined in all samples in order to include major cations for rock-matrix minerals (*e.g.*, silicates) and chemical compounds representing the original shell composition (*e.g.*, carbonates, phosphates). A box plot was made with the percentages of the chemical elements obtained in the EDS mapping of the shells. The main element percentages that compose the spinicaudata shell (Ca and P) and of the host substrate (Si and Al) were plotted to identify a relationship between the chemical compositions of the rock and of the morphological characters (STG) observed.

4. Spinicaudata abundance and richness

Ten families of spinicaudata have so far been described for the Triassic successions in Argentina (Gallego, 1992, 1996, 1999a, b, 2001, 2005, 2010; Gallego and Melchor, 2000; Gallego *et al*., 2004, 2008; Mancuso, 2005; Gallego and Martins-Neto, 2005, 2006; Tassi *et al*., 2013, 2015; Tassi, 2015). Particularly, in the LRF, the genera *Euestheria* (Euestheriidae), *Triasoglypta* (Loxomegaglyptidae), and *Triasulugkemia* (Ulugkemiidae) have been documented (Gallego 1999a,b; Gallego and Melchor, 2000; Mancuso, 2005; Tassi, 2015). Recently, Bustos Escalona (2020) described the presence of four new genera for the LRF: *Menucoestheria* (Eosestheriidae), *Cornia* (Vertexiidae), *Endolimnadiopsis* (Palaeolimnadiopseidae), and *Challaolimnadiopsis* (Pemphilimnadiopseidae). Thus, the richness of spinicaudata for this formation has been increased to 7 genera corresponding to 7 different families (Fig. 2A). On the other hand, in the AZF, the genera *Euestheria*, *Triasoglypta*, *Triasulugkemia*, and *Endolimnadiopsis* were previously described (*e.g.*, Gallego, 1999b; Gallego and Melchor, 2000; Gallego *et al*., 2001; Gallego and Martins-Neto, 2005, 2006; Tassi, 2015), whereas the genera *Dendrostracus* (Polygraptidae), *Estheriellites* (Fushunograptidae), and *Menucoestheria* were recently identified (Bustos Escalona, 2020) (Fig. 2B), increasing the richness to 7 families as well.

In the LRF, the genus *Euestheria* has a wider stratigraphic distribution when compared to other families, although it was recorded more frequently in cycles three to five (Fig. 2A). *Triasoglypta* is the second most abundant genus, although significantly less than *Euestheria*, and it is present from the second cycle onwards. The record of the other genera (*Challaolimnadiopsis*, *Endolimnadiopsis*, *Menucoestheria*, *Triasulugkemia,* and *Cornia*) is variable, ranging between cycles 2 and 5, with their best representation in cycle 3 (Fig. 2A). *Euestheria* and *Triasoglypta* remains were found together on several stratigraphic levels; however, the association of three or more genera at the same level was observed only in very few and specific sections of cycles 2 and 3. Also, particularly in cycle 3, two levels with remains of 5 and 6 genera were observed (Fig. 2A). Ten densely packed shell levels were identified along the LRF section. They are recorded in lacustrine sediments of cycles 1, 3, 4, and 5 but are more common in cycle 3 (Fig. 2A). Half of these levels are monogeneric, and the other levels include two or, in some cases, three genera.

In the AZF, the spinicaudata remains were found in the lacustrine facies (Fig. 2B). *Euestheria* is the genera with the widest distribution throughout the section, followed by *Triasoglypta*, just as in the LRF. The other genera are concentrated in the lower section of the lacustrine facies interbedded with deltaic facies and basalt flows (Fig. 2B). *Euestheria* and *Triasoglypta* genera were found together at several levels, and the record of 3 to 4 genera at the same level occurs in the lower section. The remains of *Dendrostracus* appear only in three levels, and in two of them is associated with *Euestheria* (Fig. 2B).

Twelve levels of the densely packed shells were identified along the AZF section (Fig. 2B). They are very recurrent in the lower section, where the basalt levels are interbedded. In the lower section, they include two to five genera, whereas in the upper section are generally monogeneric.

5. Taphonomy

5.1. Taphonomic grades

The remains preserved according to the TG-1 are disarticulated shells (Fig. 3A-B, D, G-J) or articulated shells (Fig. 3C) located convex-up on top of beds. On other hand, the remains preserved according to the TG-2 are shell fragments, which are generally one-third of the shells, found either as isolated remains (Fig. 3E-F) or less frequently as clusters on top of beds (Fig. 3K-L). In the LRF, the highest percentage of shells was preserved according to TG-1 (see Table S2 in the Supplemental file), with a richness of seven genera (*Euestheria, Triasoglypta, Challaolimnadiopsis, Endolimnadiopsis, Menucoestheria, Triasulugkemia, Cornia*) (Table 4). The rest of the samples were preserved according to TG-2 (*Euestheria* and *Triasoglypta*) (Table 4). In the AZF, the percentage of shells preserved according to TG-1 is lower than in the LRF, and TG-2 exceeds 40% of the total samples (see Table S2 in the Supplemental file). In the AZF, seven genera were identified for TG-1, and four genera for TG-2 (Table 4). Statistical analyses indicate that the observed percentages of TG-1 and TG-2 between formations are significantly different (see Supplemental file).

By the second taphonomic grade (STG), the remains preserved according to STG-a show most of the shells are whole (TG1) with clearly defined growth lines and remarkable ornamentation in the central zone bands. However, in the distal and umbonal zones, the ornamentation becomes diffuse (Fig. 3A-B, G-H). The shell fragments (TG2) show well-preserved morphological characters (Fig. 3E, K). In the STG-*b,* the edge of the shell is poorly differentiated, and the growth lines are delimited to a strip that covers the middle anterior, central, and middle posterior zones of the shell (Fig. 3C, F, I, L). In a few cases, the growth lines of the ventral zone cannot be distinguished. The growth bands were observed with diffuse ornamentation patterns (Fig. 3C, I). Finally, in the STG-*c*, shells with poor preservation were observed. The ventral-anterior, ventral-posterior, and ventral edges of the shell are diffuse, and the ornamentation of the bands is not visible (Fig. 3D, F, J, L).

In the LRF, STG-*a* is present in very low proportions, while STG-*b* and STG-*c* are found in similar percentages, representing almost half of the remains (Fig. 4; Table S2 in the Supplemental file). In the AZF, STG-*a* is present in a higher proportion than in the LRF, while STG-*c* is present in more than half of the samples analyzed (Fig. 4; Table S2 in the Supplemental file).

As mentioned, the mainly spinicaudata remains were recovered from horizontally laminated claystone (Fl) and mudstone, and fine-grained sandstone (SFm) of the distal lacustrine facies association. The remains collected from the lacustrine facies association are preserved according to every TG and STG for the AZF and the LRF, except STG-2*a* in the LRF. The spinicaudata remains recovered from the siltstone and sandstone (Fm/Sh) of the distal delta front facies association are preserved according to every TG and STG for the LRF, except STG-2*b*. The deltaic facies association in AZF has not recorded spinicaudata.

Both the LRF and the AZF record densely packed shell levels. The LRF shows ten levels mainly concentrated in cycles 3 to 5, with a dominance of shells preserved in TG-1, particularly in STG-*b* and STG-*c,* and scarce remains with TG-2 and STG-*a* preservation. The AZF presents twelve levels mainly concentrated in the lower section, also with the shells preserved mainly according to TG-1, STG-*b* and STG-*c*, and a few individuals corresponding to TG-2 and STG-*a*.

5.1.1. Interpretation of the taphonomic grades

Studies conducted on current spinicaudata shells show they are flexible and resistant to

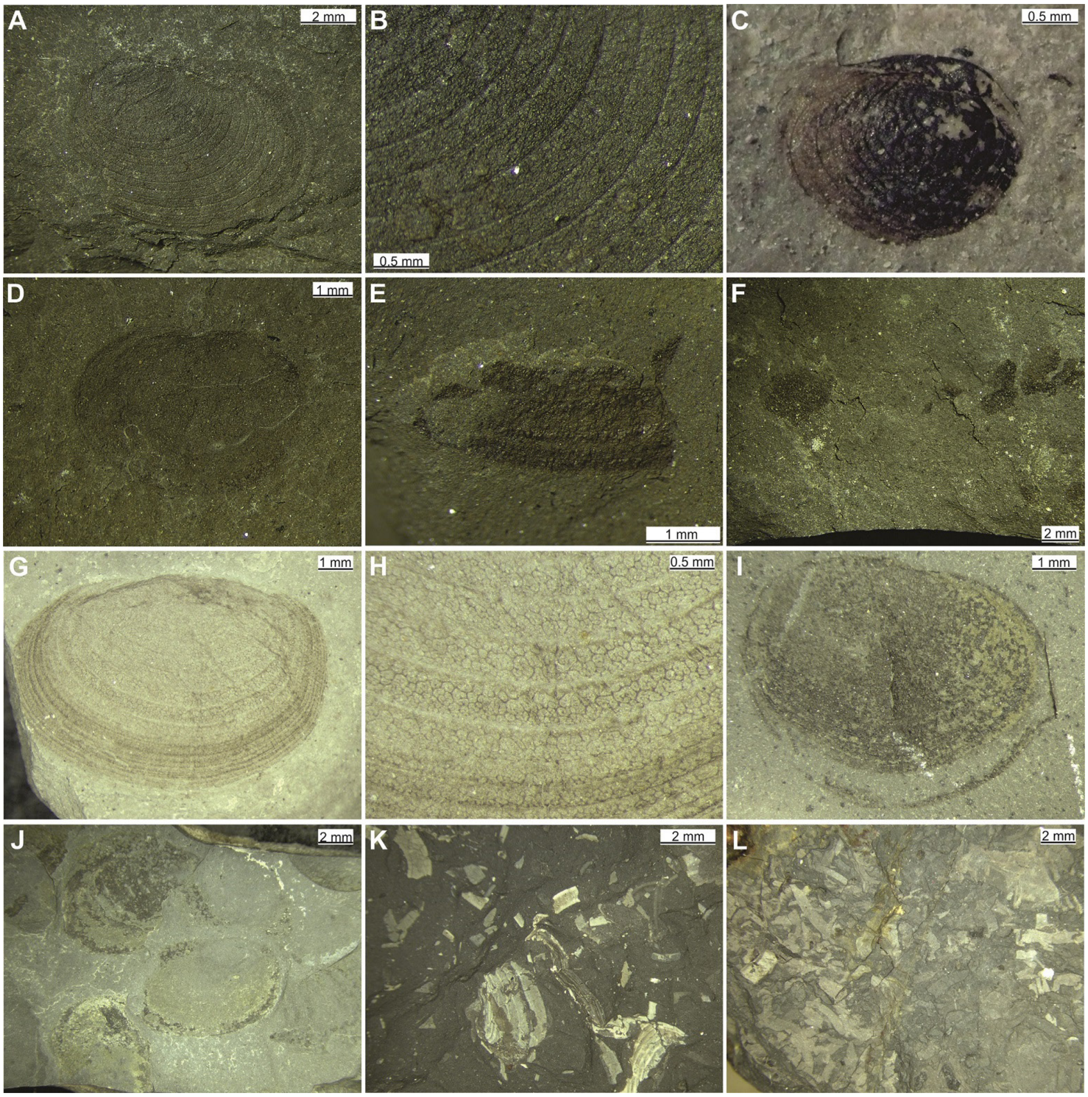

FIG. 3. Spinicaudata remains classified according to the different taphonomic grades (TG). **A-F.** Remains from the Los Rastros Formation. **A-B.** *Euestheria*; TG 1.*a*. **C.** Spinicaudata; TG 1.*b*. **D.** *Euestheria*; TG 1.*c*. **E.** *Euestheria*; TG 2.*a*. **F.** Spinicaudata; TG 2.*b* and TG 2.*c*. **G-L.** Remains from the Agua de la Zorra Formation. **G-H.** *Triasoglypta*; TG 1.*a*. **I.** Euestheriidae; TG 1.*b*. **J.** Spinicaudata; TG 1.*c*. **K.** *Triasoglypta*; TG 2.*a*. **L.** Spinicaudata; TG 2.*b* and TG 2.*c*.

destructive physical taphonomic effects in high-energy environments (*e.g.*, river transport) (*e.g.*, Astrop *et al*., 2015). However, Astrop *et al*. (2015) investigated shells reared in the laboratory, that is, under favorable confinement and controlled according to the protocol of Weeks and Zucker (1999). In addition, Astrop *et al*'s study did not contemplate periods of post-mortem spinicaudata shell dissolution (cf. Jenisch *et al*., 2017; Hu *et al*., 2020). Therefore, based on the features observed in the spinicaudata remains studied in this work, included in the TG, and according to other authors (*e.g.*, Jenisch *et al*., 2017; Hu *et al*., 2020), the degree of fragmentation of the shells can be used to interpret their habitat.

The spinicaudata remains preserved according to TG-1 are entire shells found in the Fl and Sh facies (Fig. 5). Based on the integrity of shells, we interpret that they correspond to autochthonous paleolake

TABLE 4. RECORD OF THE SPINICAUDATAN FAUNA PRESENT IN THE LOS RASTROS AND AGUA DE LA ZORRA FORMATIONS DIFFERENTIATING THE INTEGRITY GRAPH (TG) IN WHICH IT WAS FOUND.

Taxonomic level		Basin			
Suborder	Genera	Ischigualasto-Villa Unión LRF		Cuyana AZF	
		TG-1	TG-2	TG-1	TG-2
Spinicaudata	*Euestheria*	X	X	X	X
	Triasoglypta	X	X	X	X
	Triasulugkemia	X	-	X	-
	Dendrostracus	-	-	X	X
	Menucoestheria	X	-	X	-
	Endolimnadiopsis	X	-	X	-
	Challaolimnadiopsis	X	-	-	-
	Estheriellites	-	-	X	X
	Cornia	X	-	-	-

LRF: Los Rastros Formation; **AZF:** Agua de la Zorra Formation; **TG:** Taphonomic Grades; **TG 1:** entire shell; **TG 2:** fragmented shell.

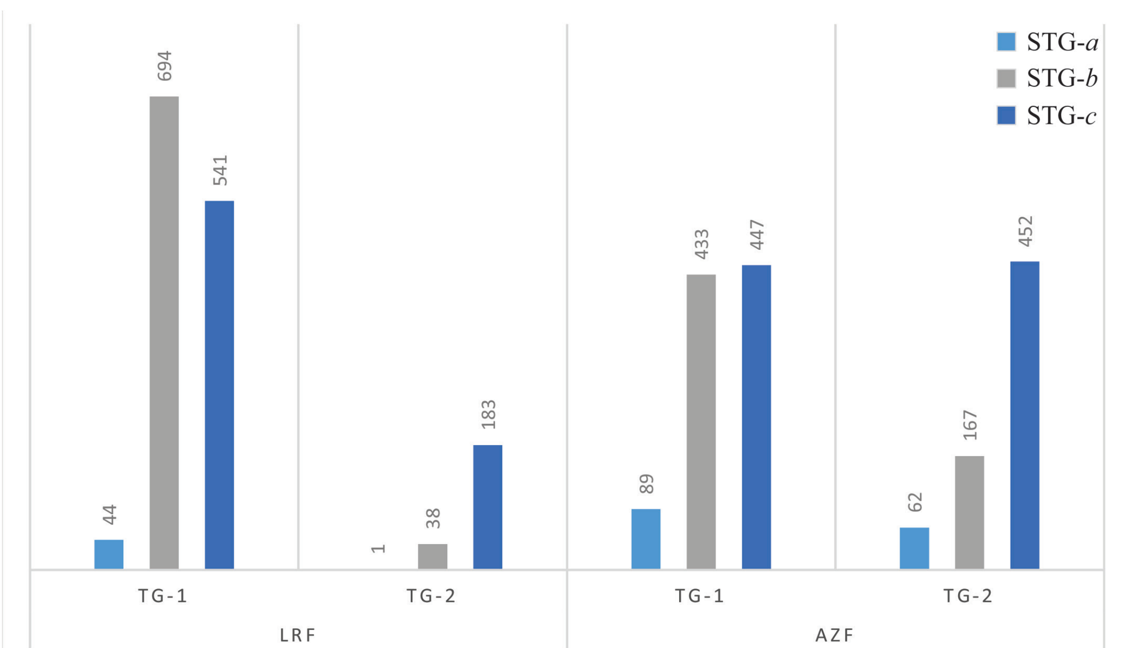

FIG. 4. Abundance of spinicaudata shells identified according to taphonomic grades (TG-1,2) and second taphonomic groups (STG-*a, b, c*) in the Los Rastros Formation (LRF) and the Agua de la Zorra Formation (AZF).

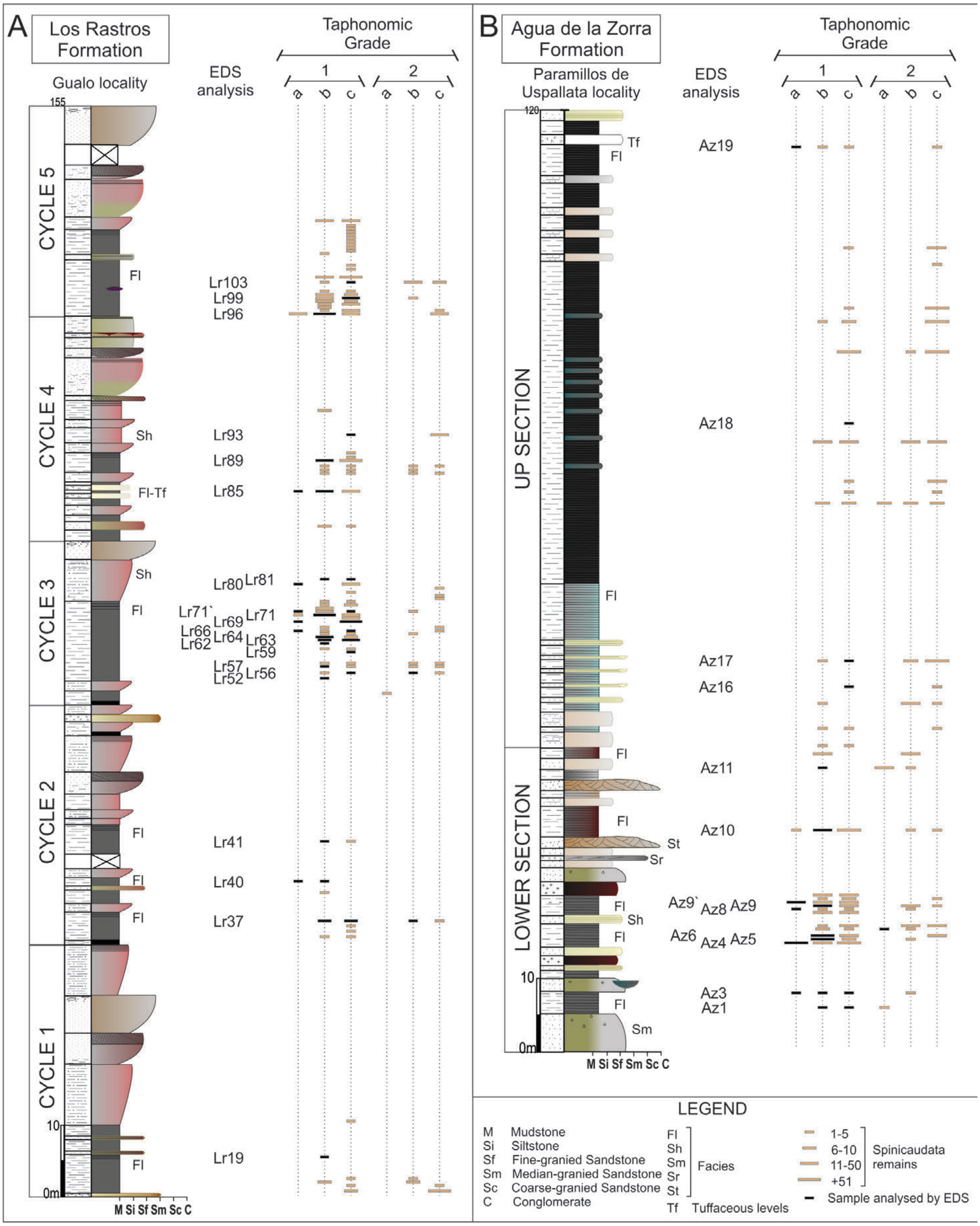

FIG. 5. Stratigraphic distribution of the different spinicaudata taphonomic grades and location of samples analyzed by energy-dispersive X-ray spectrometry (EDS). **A.** The Los Rastros Formation, **B.** The Agua de la Zorra Formation.

spinicaudatans, inhabiting the calm and sheltered margin of the lake and sheltered delta zone. The recently dead animals were likely transported by the natural circulation of the lake from the inhabited zone to the open water, where they sank to the lake bottom or distal delta front layers.

The TG-2 reveals a more complex history due to the two distinct fracture types recognized. The shell fragments, characterized by sharp or marked fractures with well-defined edges, suggest episodes of predation or scavenging by the fish that inhabited the paleolake (*e.g*., McKenzie, 1981; Mancuso and Marsicano, 2008). The remains preserved according to TG-2 with sharp fractures are found in Fl of the distal lacustrine and Fm/Sh of the distal delta front facies association (Fig. 5). Based on this evidence, we interpret that the remains correspond to autochthonous paleolake spinicaudatans, inhabiting the margin zone, and the fragment arrived to the lake bottom and distal delta front layers after predation or scavenging episodes. On the other hand, spinicaudata remains fragmented following the weak zones of the shell (growth lines) were recorded in the Fl of the distal lacustrine (TG-2 and STG-b and STG-c), and Fm/Sh of the distal delta front facies association (STG-c) (Fig. 5). The exposure of the shells at the sediment-water interface after death favors the dissolution process of the outer layers (see Hu *et al*., 2020). Thus, the weakened shells become susceptible to break when they are subjected to mechanical forces (*e.g*., flow transport) (Brett and Bair, 1986; Plotnick, 1986; Farinati and Zavala, 1995; Fernández-López, 2000; Bustos Escalona *et al*., 2017; Jenisch *et al*., 2017; Hu *et al*., 2020). Based on the weakened fractures, we interpreted that these remains correspond to allochthonous spinicaudatan, possibly inhabiting ponds upstream of the paleolake. The shells, after death, were exposed for some time at the sediment-water interface, and were then transported to the paleolake, where they sank to the lake bottom and distal delta front layers.

The second taphonomic grade (STG) is characterized by the integrity of shell morphological characters. The different grades represented from STG-*a* to STG-*c* show a progressive loss of morphological character integrity (Table 3). Based on the dissolution process suffered by shells during exposure at the sediment-water interface (Hu *et al*., 2020), we interpret that remains included in STG-*a* were buried relatively quickly after death, experiencing a short time at the sediment-water interface (Krishnan, 1958; Brett and Baird, 1986; Mancuso and Gallego, 2000; Cohen, 2003; Jenisch *et al*., 2017; Hu *et al*., 2020). The remains preserved according to STG-*b* show diffuse edges, growth lines, and ornamentation (Table 3; Fig. 3F, L). Based on the moderate loss of morphological features, we interpret that these spinicaudata remains underwent a moderate time of exposure at the sediment-water interface in the aqueous environment after death, which favored the dissolution of the edge of the shell (Brett and Baird, 1986; Mancuso and Gallego, 2000; Birggs, 2003; Mancuso and Marsicano, 2008; Astrop *et al*., 2015; Jenisch *et al*., 2017; Hu *et al*., 2020). Particularly, the shell fragments preserved according to STG-*b*, which show fractures in the weak zones (growth lines) of the shell and with diffuse growth bands, show that the shells experienced dissolution after death in the ponds upstream of the paleolake, weakening the shell and favoring fragmentation during transport (Driscoll, 1970; Driscoll and Weltin, 1973; Seilacher *et al*., 1985; Brett and Baird, 1986; Mancuso and Gallego, 2000; Jenisch *et al*., 2017; Hu *et al*., 2020). Finally, the specimens included in STG-*c* did not preserve morphological characters. They represent both autochthonous (TG-1) and allochthonous (TG-2) individuals, exposed for a long time at the water-sediment interface before their final burial, either in ponds, or in the paleolake.

5.2. Chemical analyses

Seventy-one samples selected for SEM-EDS analysis were collected from the Fl of the distal lacustrine (67 samples) and Fm/Sh of the distal deltaic front (4 samples) facies association from different stratigraphic levels along the LRF and the AZF sections (Fig. 5). EDS maps of the spinicaudata remains show trends in elemental distributions. EDS allowed the recognition of several elements, but only the main elements composing the shell (P, Ca) and the host rock (Si, Al) are shown in Table 5. The EDS results show, in both formations, a general trend with the main concentration of Ca and P in the shell zone in contrast to the main concentration of Si and Al in the matrix zone (Fig. 6). They also show that the concentration of the original shell components (Ca and P) decreases from STG-*a* to STG-*c*, so the distribution of Ca and P in STG-*c* is more homogeneous between shell and matrix than in STG-*a* and STG-*b* (Fig. 6; Table 5).

TABLE 5. MAJOR ELEMENT COMPOSITION DATA (O, AL, SI, K, P AND CA).

Formation	Log section	Sample	Spinicaudata Genera	SGT	O	Al	Si	K	P	Ca
Los Rastros	C 1	LR19-1	*Euestheria*	b	51.79	7.3	23.72	3.44	0.11	n.d.
	C 2	LR37-2	*Triasoglypta*	b	37.96	4.75	14.76	2.11	5.56	13.48
		LR37-21	*Triasulugkemia*	b	44.3	2.79	9.24	1.02	7.64	16.57
		LR37-3	*Euestheria*	c	39.61	4.62	13.57	1.98	5.45	12.78
		LR37-4	*Euestheria*	b	39.63	7.34	23.53	3.82	1.15	2.98
		LR37-41	*Euestheria*	b	36.29	5.92	18.69	3.09	2.02	5.13
		LR37-5	*Euestheria*	c	40.91	7.06	23.56	3.8	0.76	1.97
		LR37-7	*Euestheria*	b	47.02	6.33	17.64	2.63	2.07	4.49
		LR40-1	*Triasoglypta*	b	45.41	9.21	18.25	3.14	0.26	0.32
		LR40-2	*Triasoglypta*	b	47.64	7.97	18.16	3.51	0.05	2.97
		LR41-1	*Euestheria*	b	38.61	4.95	10.95	1.32	n.d.	5.66
	C 3	LR52-1	*Euestheria*	b	33.34	6.16	15.41	1.77	1.37	4.05
		LR56-3	*Euestheria*	c	43.63	7.71	23.46	2.98	0.15	0.34
		LR56-6	*Euestheria*	b	43.47	9.1	24.57	3.22	0.14	0.37
		LR57	Spinicaudata	b	40.78	7.27	21.89	2.78	0.21	0.26
		LR59-1	Spinicaudata	c	30.09	6.14	16.09	2.13	n.d.	0.57
		LR62-3	Spinicaudata	b	40.02	6.74	16.49	2.06	0.07	0.19
		LR63-3	*Euestheria*	b	32.9	4.62	12.86	1.63	0.16	0.9
		LR63-4	*Euestheria*	b	28.88	5.81	19.31	2.78	0.75	2.02
		LR63-5	*Euestheria*	b	43.1	7.91	23.44	2.95	0.94	2.29
		LR63-6	*Challaolimnadiopsis*	c	39.43	5.7	15.85	2.16	0.11	0.31
		LR63-7	*Menucoestheria*	c	29.66	5.7	15.84	2.1	0.31	0.91
		LR63-8	*Triasulugkemia*	b	40.41	7.65	22.36	3.07	0.19	0.58
		LR64-1	*Triasoglypta*	b	31.6	6.06	17.67	2.38	1.97	5.04
		LR64-10	*Triasoglypta*	b	32.28	4.95	16.58	2.03	0.32	0.7
		LR66-4	*Euestheria*	a	37.04	6.45	19.96	2.27	0.86	2.09
		LR66-5	*Endolimnadiopsis*	a	42.28	7.88	19.87	2.42	n.d.	0.23
		LR69-2	*Euestheria*	c	33.86	5.66	17.52	2.47	0.14	0.63
		LR69-4	*Cornia*	a	31.17	4.41	18.07	2.38	0.41	1.4
		LR69-5	*Euestheria*	a	36.04	6.55	19.97	2.38	0.42	0.69
		LR71-1	*Euestheria*	b	39.65	8.02	23.42	3.28	2.01	0.46
		LR71-3	*Euestheria*	b	36.41	6.8	21.14	3.24	2.54	4.93
		LR71-4	*Euestheria*	b	41.58	7.99	22.59	2.8	0.32	0.63
		LR71-5	*Euestheria*	b	39.82	7.01	20.06	2.64	0.45	0.49
		LR71-6	*Euestheria*	b	34.77	6.69	21.92	3	1.16	3.08
		LR71-7	*Euestheria*	b	35.73	5.62	15.31	2.02	1.88	4.51
		LR71-8	*Euestheria*	b	35.68	6.42	18.6	2.57	0.93	2.45
		LR71`-1	*Euestheria*	a	39.47	3.8	12.89	13.77	7.45	0.28

table 5 continued.

Formation	Log section	Sample	Spinicaudata Genera	SGT	O	Al	Si	K	P	Ca
Los Rastros	C3	LR71`-2	*Euestheria*	c	33.88	5.82	17.12	2.11	n.d.	n.d.
		LR80	*Euestheria*	a	41.21	4.11	12.26	1.85	7.99	15.37
		LR81-1	*Euestheria*	c	35.65	3.81	11.7	1.39	0.18	0.4
		LR81-2	*Euestheria*	b	25.04	3.38	10.77	1.4	0.54	0.81
	C 4	LR85-1	*Euestheria*	b	46.38	7.91	29.37	3.26	n.d.	n.d.
		LR85-1	*Euestheria*	a	30.51	5.23	18.91	1.95	n.d.	0.28
		LR85-2	*Euestheria*	a	7.02	2.78	11.75	1.43	n.d.	n.d.
		LR85-3	*Euestheria*	a	36.84	6.11	22.01	2.28	n.d.	0.45
		LR89	*Endolimnadiopsis*	b	9.24	1.25	3.47	0.38	n.d.	0.21
		LR93	*Euestheria*	c	8.71	1.25	4.53	0.48	n.d.	0.3
	C 5	LR96	*Euestheria*	b	42.15	9.39	21.24	2.69	1.52	3.69
		LR96-2	*Euestheria*	b	43.8	8.02	22.33	2.94	0.23	1.38
		LR99	*Euestheria*	c	45.57	9.61	22.28	2.76	0.53	1.23
		LR103	*Euestheria*	c	43.16	8.6	21.03	2.76	n.d	n.d
Agua de la Zorra	Lower section	AZ1-1	Spinicaudata	c	33.73	5.13	14.57	1.35	0.95	5.04
		AZ1-2	*Estheriellites*	b	39.79	5.39	14.34	1.5	2.97	7.77
		AZ3-1	*Euestheria*	c	42.16	4.73	22.12	3.31	2.46	6.96
		AZ3-2	*Endolimnadiopsis*	b	39.9	5.34	22.59	3.62	1.25	4.11
		AZ4	*Euestheria*	a	39.33	5	18.44	3.39	1.33	7.8
		AZ5-1	*Endolimnadiopsis*	b	43.65	2.97	10.37	2.21	7.62	18.83
		AZ5-2	Spinicaudata	b	42.15	2.49	8.51	1.99	9.6	24.21
		AZ6	*Euestheria*	b	45.95	5.93	24.68	4.36	1.09	3.8
		AZ8	*Triasoglypta*	a	41.49	7.41	22.87	5.96	0.7	2.92
		IANIGLA-PI:3126	*Triasoglypta*	b	37.68	8.87	17.51	1.94	0.11	1.59
		AZ9-2	*Endolimnadiopsis*	b	43	10.16	20.28	2.02	n.d.	1.17
		AZ9`	*Endolimnadiopsis*	a	41.09	7.73	19.78	3.85	2.36	n.d.
		AZ10	*Triasulugkemia*	b	37.36	4.71	18.45	2.02	3.66	8.36
		AZ11	*Dendrostracus*	b	41.89	8.2	28.27	3.14	0.7	0.27
		AZ16	*Euestheria*	c	41.79	9.26	21	3.45	n.d.	0.5
	Upper section	AZ17	*Euestheria*	c	33.73	5.92	19.56	2.08	n.d.	0.82
		AZ18-1	*Euestheria*	c	41.35	6.6	19.3	2.13	0.1	0.32
		AZ18-2	*Euestheria*	c	30.27	5.45	16.37	1.83	0.2	0.46
		AZ19	*Dendrostracus*	a	39.76	6.54	20.74	2.12	0.2	0.15

Major element composition data (O, Al, Si, K, P and Ca) from 71 samples, 52 samples from the Los Rastros and 19 samples from the Agua de la Zorra formations. All measurements are expressed in weight percentage (wt%) **C:** cycle, **SGT:** Second level taphonomic grade, **n.d.:** not detected.

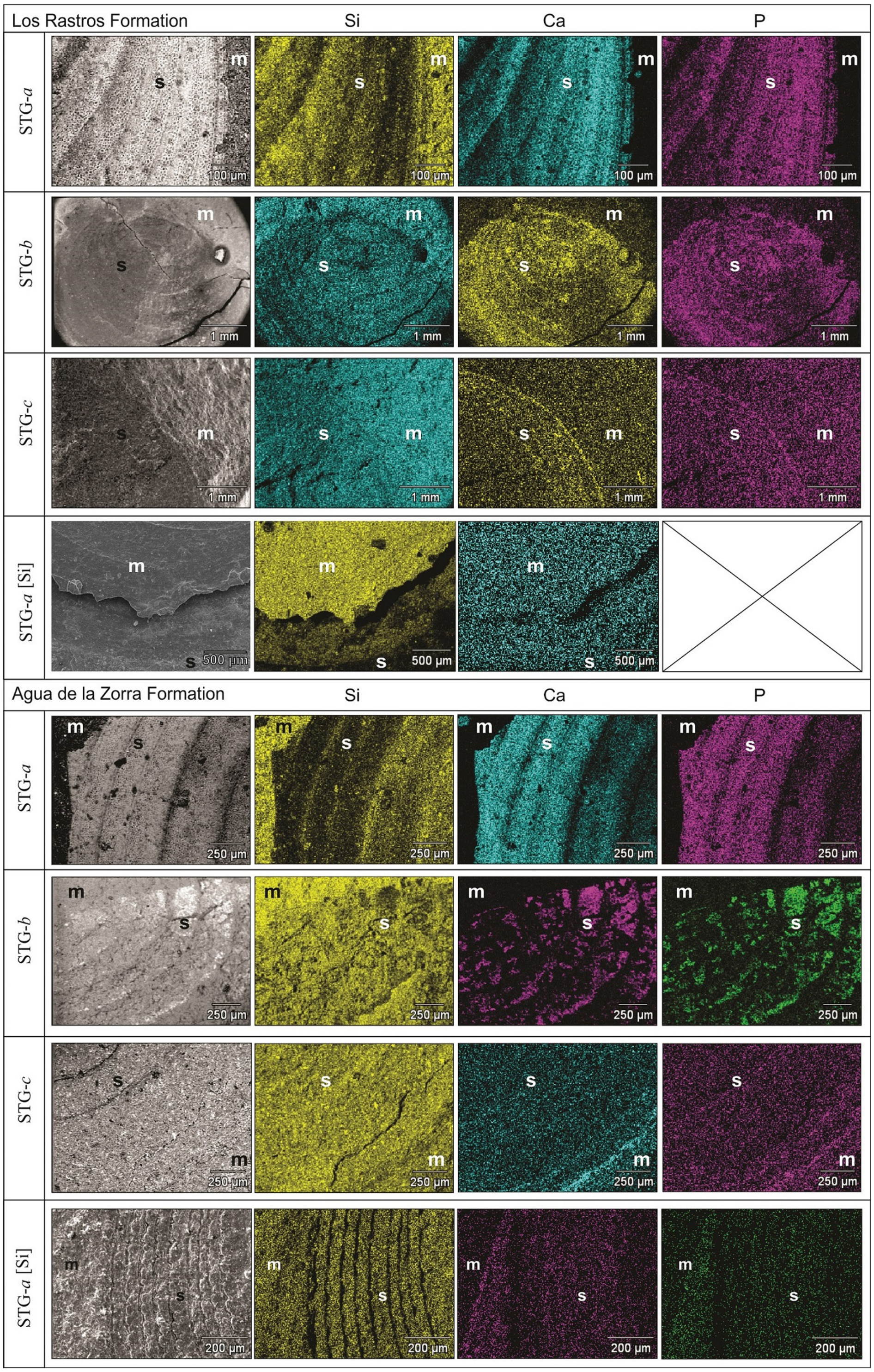

FIG. 6. EDS maps (Si, Ca, and P) for the spinicaudata shells (**s**) and host rocks (**m**) according to the second taphonomic grades (STG) in the Los Rastros Formation and the Agua de la Zorra Formation. STG *a* - [Si] example of a well preserved and silicified shell. **Si:** silica; **Ca:** calcium; **P:** phosphorus.

The box plots (Fig. 7) highlight the particularities of the trends observed in both the LRF (Figs. 7A-B) and the AZF (Fig. 7C-D). The LRF samples, especially in the Fl of the distal lacustrine facies association of cycles 1, 2, 3, and 5, show differences in the Si, Al, Ca, and P concentrations in each STG (Fig. 7A), with higher, Ca and P concentrations in the shells for STG-*a* (Figs. 6, 7A). However, the samples LR85-1, LR85-2, and LR85-3, that were found also in the Fl of the distal lacustrine facies association but between the tuff levels of cycle 4 (Fig. 5), record a higher Si concentration, lowest Ca concentration, and absence of P in the shells.

The samples preserved in Fm/Sh of the distal delta front facies association: LR80 according to STG-*a*, LR81-1 according to STG-*c*, LR81-2 according to STG-*b* (cycle 3), and LR93 according to STG-*c* (cycle 4), also show higher Ca values than Si (Table 5) in the shell for STG-*a* and the lowest Ca and P concentration, with a higher and more homogeneous Si concentration, in the shell and in the rock matrix around the shell for STG-c (Table 5; Figs. 5, 6).

In the AZF, the box plots show that Ca, P, Si, and Al concentrations in the shell zone are as diverse as in the LRF lacustrine facies samples (Table 5; Fig. 7C). As occurs in the LRF, a higher concentration of Ca and P is observed in the samples of the Fl of the distal lacustrine facies association from the AZF upper section for the STG-*b* samples compared to the STG-*c* samples, which present higher concentration of

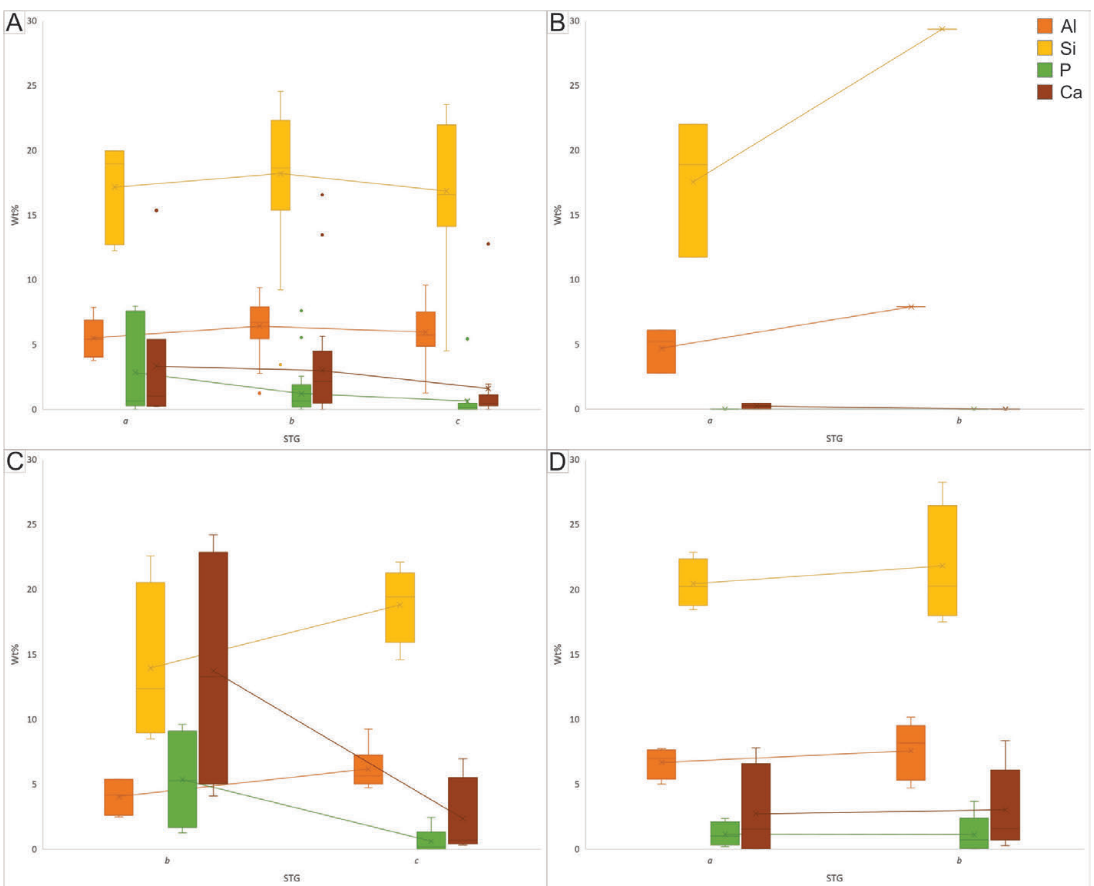

FIG. 7. Box plot showing the weight percentage (wt%) of the main components that make up the rock matrix (Si and Al) and the shell (Ca and P) for the different STGs. **A.** Box plot of samples corresponding to paleolake sections without volcanic influence in the LRF. **B.** Box plot of samples corresponding to paleolake sections with volcanic influence in the LRF. **C.** Box plot of samples corresponding to paleolake sections without volcanic influence in the AZF. **D.** Box plot of samples corresponding to paleolake sections with volcanic influence in the AZF.

Si and Al in the preserved zone of the shell (Figs. 6, 7C). Moreover, sample AZ19, preserved according to STG-*a* from Fl of the distal lacustrine facies association, but between tuff levels (Tf) (Fig. 5B), shows elevated Si and Al concentrations (Table 5). In the AZF lower section, samples preserved according to TG-1, STG-*a,* and STG-*b* (AZ1-AZ9`) are found in Fl of the distal lacustrine facies association below the basaltic flow level (Fig. 5B) and show a higher Si and Al concentration in the shell zone (Table 5).

5.2.1. Interpretation of the chemical analysis

The comparison of the general trend of the three STG for the LRF and the AZF suggests a relationship between the decreasing Ca and P concentration and the integrity of the morphological characters (Figs. 6, 7). The longer time exposed at the water-sediment interface that the shells underwent favored not only the loss of morphological characters but also the dissolution of the original shell components (Ca and P) (Golubic and Schneider, 1979; Behrensmeyer *et al*., 2000; Briggs, 2003; Cohen, 2003; Hu *et al*., 2020).

The variations in the general trends in lacustrine samples are similar between both formations. The LRF and the AZF (upsection) lacustrine samples show the best original component preservation (Fig. 7A), with a clearer trend in the AZF lacustrine samples (upsection) that show an increase of Si in shell and matrix areas with a decrease of Ca and P (Fig. 7C). This observation suggests that the Fl of the distal lacustrine deposits favored the preservation of the original component (Fig. 5, 7A, 7C; Table 5) (Behrensmeyer and Hook, 1992; Behrensmeyer *et al*., 2000; Cohen, 2003; Hu *et al*., 2020). In distal delta front samples of the LRF, the concentration of the original components of the shell (Ca and P) decreases from STG-a to STG-c, while the concentration of the matrix components (Si and Al) increases. Furthermore, these matrix components become homogeneously distributed in the shell area (Fig. 7A; Table 5).

As mentioned above, both paleolakes recorded volcanic influence, which were likely to affect the preservational condition of shells. Some authors proposed that the alkaline microenvironment, produced by volcanic ash input and decomposition of the volcanic glass particles, can promote phosphate precipitation (*e.g*., Berner, 1968; Gulbrandsen, 1969; Allison, 1988; Hu *et al*., 2020), one of the most important biomineralization component of the spinicaudatan shells (Klug *et al*., 2005; Stigall and Hartman, 2008; Astrop, 2014). However, the decay of the shells decreases the pH of the microenvironment around them, and the emission of CO_2 by volcanic processes increases the water acidity, inhibiting the precipitation of phosphate (Gabbott, 1998; Briggs, 2003; Hu *et al*., 2020). In both paleolakes, the shells interbedded with basalt flow levels (AZ1-AZ9`, AZ19) or ash fall (AZ19) in the AZF, and that from the LRF cycle 4 (LR85) show a decrease or even absence of the original component (Ca and P) in favor of Si (Table 5), resulting in almost an entire silicification of the remains (STG-*a* and STG-*b*) (Fig. 5). This evidence suggests that in both paleolakes, the alkalinity produced by volcanic influence could be neutralized at least in the microenvironment around shells by their decay and by the emission of CO_2 that produces a decrease in pH, inhibiting the phosphatization and favoring the silicification (Hu *et al*., 2020).

6. Stratigraphic distribution and taphonomic history of spinicaudatans

6.1. Los Rastros Formation

In the LRF, the stratigraphic distribution and TG of the spinicaudata taxa (Figs. 2A, 5A), show an evident change in abundance and richness between cycles 1-2 and cycles 3-5. During cycles 1 and 2, the presence of individuals mainly of TG-1 in Fl facies indicates the autochthony of the spinicaudata to the main water body, inhabiting the coasts and oxygenated areas of the paleolake (Fig. 5A) as postulated by Mancuso and Marsicano (2008). Both cycles preserved a few specimens included in TG-1 (Sh facies) and TG-2 (Fl facies), suggesting the transport of spinicaudata by tractive flows that incorporated shell remains into the main water body, indicating a low input of allochthonous spinicaudata (Fig. 5A) (Mancuso and Marsicano, 2008). Also, in both cycles, *Euestheria* is the most common taxon, followed exclusively in cycle 2 by *Triasoglypta* and *Triasulugkemia* (Fig. 2A).

During the transition between cycles 2 and 3, a second half-graben controlled independently by a secondary fault was proposed based on the sedimentological evidence, the architectural patterns, stratigraphic and paleogeographic distribution of the deposits, and source areas at the Gualo-Chañares area

(Mancuso and Caselli, 2012; Benavente *et al.*, 2021). Thus, it resulted in a division of the major Los Rastros paleolake and the development of a smaller isolated paleolake in the Gualo-Chañares area (Mancuso and Caselli, 2012). Pedernera *et al.* (2020) suggest that the decrease in plant taxa recorded between cycles 3-4 would be related to a change or reduction of input areas resulting from the isolation suffered by the activity of a secondary fault. From a taphonomic point of view, the recorded increase of spinicaudatans taxa and the increase of remains in cycle 3 (Fig. 2A) could be correlated with changes in the LRF paleolake for the Gualo-Chañares area resulting from this tectonic event. Cycle 3 shows the highest abundance and taxa richness. There is a high increase in the richness and abundance of paleolake autochthonous spinicaudata (TG-1, Fl facies) and a moderate increase in abundance of the allochthonous spinicaudata (TG-2, Fl and Sh facies). This cycle preserved multi-taxa levels with up to six different taxa together (Fig. 2A). The presence of multi-taxa levels suggests the main paleolake included a variety of subenvironments and limnological conditions (*e.g.*, pH, temperature, salinity, vegetation) for the development of diverse spinicaudata assemblages within the trophic zones (Kapler, 1960; Petr, 1968; Royan, 1976; Orr and Briggs, 1999; Dumont and Negrea, 2002). Even in a few meters, four events of the densely packed shells are concentrated with equal preservation grade, suggesting a sudden change in the limnologic parameters, such as pH, nutrients, and/or solute concentration, resulting in unfavorable conditions to the growth of the spinicaudata assemblages (Kapler, 1960; Baird, 1862; Klunzinger, 1864; Bishop, 1967; Petr, 1968; Royan, 1976; Gislén, 1937; Massal, 1954; Tasch and Zimmerman, 1961; Moore, 1965; Horne, 1967; Mancuso and Marsicano, 2008).

Cycle 4 shows a decrease of almost half of the spinicaudata richness and abundance compared to cycle 3 (Fig. 2A). The autochthonous spinicaudata (TG-1) continues to be dominant in the assemblage (Fig. 7A) with a low abundance of allochthonous specimens (TG-2). Surprisingly, *Triasoglypta* is absent in this cycle, with an absolute dominance of *Euestheria* with a few representatives of *Endolimnadiopsis, Menucoestheria*, and *Triasulugkemia* (Fig. 2A). This cycle includes several ash levels interbedded with distal lacustrine facies rich in autochthonous spinicaudata (TG-1) (Figs. 2A, 7A). The relation between the ash fall levels with the increase of spinicaudatan specimens suggests a volcanic influence in chemical limnological parameters, but not enough to produce a mortality event. One densely packed shell level is preserved in cycle 4 close to the distal delta front facies (Fig. 2A). The event includes autochthonous spinicaudata in an excellent state of preservation (TG-1) (Mancuso and Marsicano, 2008). Therefore, the physical factors that generated this shell packing occurred in the main paleolake. The allochthonous specimens (TG-2) were found in sediments at the distal delta front, evidencing the input of spinicaudata remains from ponds upstream from the main paleolake (Mancuso and Marsicano, 2008).

Finally, cycle 5 shows an increase in the spinicaudata abundance, approximately twice as much as in cycle 4, while the richness keeps on low (Fig. 2A). The most abundant spinicaudatan remains, in facies Fl, are considered autochthonous specimens (TG-1) with good preservation, while a small percentage are allochthonous specimens (TG-2). As occurred in the rest of the unit, *Euestheria* is the most abundant taxa, followed by *Triasoglypta*, and in this cycle *Endolimnadiopsis* is observed (Fig. 2A). Three densely packed shell levels were found in this cycle dominated by autochthonous spinicaudata. Two of these preserved the shells on distal lacustrine deposits (Fl facies), and the last on turbidity flow deposits (SFm facies) (Table 1) that probably removed the death spinicaudatan remains previously deposited on the deltaic front. These spinicaudata are considered autochthonous to the deltaic environment (Mancuso and Marsicano, 2008).

6.2. Agua de la Zorra Formation

The AZF unit was divided into two sections, the lower section included the interbedded distal lacustrine facies with delta facies and basalt lava flows, and the upper section represented the distal lacustrine deposits. The lower section concentrated the highest abundance and taxa richness for the unit (Fig. 2B). The highest concentration of the autochthonous spinicaudata (TG-1) is between basalt lava flows (Fig. 7B), although these levels also concentrated most densely packed shells (Fig. 2B). The recorded volcanic activity could have modified the physical conditions (temperature and spatial reduction of habitat) in the short term, as well as in the long-term chemical conditions (pH, salinity) of the paleolake

(Behrensmeyer and Hook, 1992; Fürsich and Pan, 2015; Hu *et al*., 2020). Also, the lower section levels are bearing multi-taxa assemblage suggesting a variety of subenvironments and limnologic conditions that favored the development of complex spinicaudatan assemblages within the trophic zones (Kapler, 1960; Petr, 1968; Royan, 1976; Orr and Briggs, 1999; Dumont and Negrea, 2002). We believe that the recurrent fluctuations in limnological parameters alternately favored and/or disfavored the growth of the spinicaudatan assemblages.

The upper section shows a lower abundance and taxa richness (Fig. 2B), with a similar number of autochthonous (TG-1) and allochthonous (TG-2) spinicaudata (Fig. 7B). The record of only one level of densely packed shells (AZ19), with the lower taxa richness and mono-taxa levels (Figs. 2B, 5B), suggests a stable water body with a low variety of subenvironment and limnologic conditions that favored the development of monospecific spinicaudatan assemblages.

7. Comparison of Los Rastros and Agua de la Zorra formations

The LRF and the AZF share five spinicaudata taxa (Table 4), two of which are autochthonous and allochthonous (*Euestheria* and *Triasoglypta*). The presence of the genera *Euestheria, Triasoglypta, Triasulugkemia, Menucoestheria,* and *Endolimnadiopsis* as autochthonous paleofauna in the Los Rastros and Agua de la Zorra paleolakes, indicates that the limnologic conditions in the trophic zones of the main water bodies were in the ecological range for the development of these groups of taxa. Both the LRF and the AZF recorded the genera *Euestheria* and *Triasoglypta* as allochthonous paleofauna too, suggesting that the inhabited ponds also presented limnologic conditions in the ecological range that favored their development.

The autochthonous spinicaudata taxa unique to each formation (*Cornia* and *Challaolimnadiopsis*) (Table 4) are recorded in the multi-taxa assemblage (Fig. 2A). These findings are interpreted as the result of the development of complex spinicaudata assemblages, which are associated with the diverse subenvironments and limnological conditions within the trophic zone. The genera *Cornia* is widely recorded in the Lower Triassic of India (Ghosh *et al*., 1987a, b; Ghosh, 2011), Germany (Kozur and Seidel, 1983a, b; Kozur, 1993; Bachmann and Kozur, 2004; Kozur and Weems, 2007, 2010), Early Triassic of Russia (Novojilov, 1970), and Australia (Tasch, 1987), the Upper Triassic of Africa and Brazil (Tasch, 1987). The larger forms are most common in the Lower Triassic of South America (Ghosh and Dutta, 1996; Ghosh, 2011; Tassi *et al*., 2013). This genus, in Argentina, has been recorded in the Middle Triassic (Tassi *et al*., 2013; Tassi, 2015). The small size of specimens of the genera *Cornia*, and the presence of the umbonal spine in this taxon, has been proposed as an indicator of arid environments, prone to drying out, and of water bodies with high salinity (Tasch, 1963; Ghosh, 1980, 1984; Ghosh and Dutta, 1996). The genera *Challaolimnadiopsis* has been recorded in Argentina in the Cerro de las Cabras Formation (Middle Triassic) and the Potrerillos Formation (Middle to Early Upper Triassic) in the Mendoza province (Shen *et al*., 2001; Tassi, 2015). *Challaolimnadiopsis* remains have been recorded in low energy and/or stable environments under semi-arid seasonal climate conditions (Tassi, 2015). Both taxa (*Cornia* and *Challaolimnadiopsis*) have been recorded as autochthonous spinicaudata in Fl facies on Cycle 3 in the LRF (Table 4; Fig. 2A). There is no evidence of arid or desiccation conditions in the LRF at the Gualo area; moreover, the multiproxy climatic analyses of the LRF support that it was a humid environment (Mancuso *et al*., 2020). Therefore, *Cornia* and *Challaolimnadiopsis* are probably opportunistic taxa that can inhabit more environments.

The genera *Estheriellites* and *Dendrostracus* were only recorded in sediments from the AZF paleolake as autochthonous and allochthonous specimens (Fig. 2B; Table 4). *Estheriellites* is a genus that registers only two species for the Triassic in Argentina (Gallego, 1999b, 2001; Tassi, 2015) inhabiting a stable low-energy lake environment (Tassi *et al*., 2015). The genus *Dendrostracus* has been previously described for the Upper Triassic (Tassi, 2015) and Lower Cretaceous of Argentina (Pramparo *et al*., 2005), and the Middle Jurassic of Scotland (Chen and Hudson, 1991). Individuals in this genus have been associated with semi-permanent to ephemeral shallow lake deposits associated with river systems (Chen and Hudson, 1991; Pramparo *et al*., 2005). However, Tassi (2015) associates it with spinicaudata assemblages of the permanent lake, as they are found without transport marks in distal lacustrine sediments, along with individuals of the genus *Triasoglypta*. In our study, *Estheriellites* shells were found only in the lower section of the AZF. These remains were preserved as TG-1 STG-*b* and TG-2 STG-*a*. On the other hand, remains assigned to *Dendrostracus*, preserved as TG-1 STG-*a* and TG-2 STG-*b*, were identified in the lower section of the AZF (distal lacustrine facies). Also, *Dendrostracus* remains, assigned to TG-1 STG-*a*, were recorded in the upper section of the AZF (Fig. 2B; Table 4). As mentioned above, the AZF paleolake is characterized as a deltaic environment with evidence of volcanic activity, suggesting that conditions in the trophic zones and areas surrounding the paleolake were not stable in the long-term (Pedernera *et al*., 2021). The record of the genera *Estheriellites* and *Dendrostracus* is interpreted here as autochthonous and allochthonous elements, suggesting that life assemblages of these genera could have exhibited a wide tolerance to environmental factors, being able to inhabit and develop also in disturbed environments.

The large number of levels with densely packed shells, in both formations, suggests an increased mortality possibly related to abrupt environmental changes that modified the conditioning factors for the development and growth of spinicaudata paleofauna and the area of inhabited space (Mancuso and Marsicano, 2008). While in the AZF, the recurrent fluctuation in the paleolimnological parameters that are the source of increased mortality is mainly concentrated around the basaltic lava levels of the lower section, in the LRF this fluctuation is not linked to significant volcanic episodes.

As mentioned above, EDS and box plot graphics show a relationship between the loss of morphological character integrity and the decrease in the concentration of original components (Ca and P) of the spinicaudata shells (Figs. 6, 7; Table 5). P is an element considered a limiting factor for life development in lake systems (*e.g.*, Schindler, 1977; Wetzel, 2001; Sterner, 2008). The concentration of P in living spinicaudatan shells depends on the concentration of dissolved P in the lake system (Stigall *et al*., 2008; Astrop *et al*., 2015). Likewise, a lake system with low P concentration tends to rapidly dissolve P from dead organisms, increasing the level of dissolved P in the lake system (Warren, 1986). The high Si percentages in shells preserved according to STG-*b* and STG-*c* in both formations suggest that both paleolakes contained water poor in available dissolved P, making silicification the main diagenetic process in the fossilization of spinicaudata shells (Hu *et al*., 2020). However, the distal lacustrine facies (Fl) of the upper section of the AZF records a lower P concentration than the distal lacustrine facies (Fl) of the LRF, suggesting different diagenetic conditions and dissolved P concentration in the water.

Si is the component representative of the rock matrix, replacing the original shell components. Si-rich waters can favor the silicification process by directly interacting the organic remains with microbial mats (Konhauser *et al*., 2001). However, in the Triassic paleolakes studied here, the shells with the highest concentration of Si are associated with volcanic activity. Therefore, the high Si concentrations in the shells could have been favored by the high Si contribution to the system through volcanic ash supply, basalt lava flows, and/or volcanic fluids (Renaut *et al*., 2002, 2012; Mancuso *et al*., 2010; Benavente *et al*., 2014). The SEM images and EDS results suggest that in both formations, the preserved shells with high Si concentrations are mainly molds of the external layer of the shells. Only a few shells were subjected to mineralization processes of volcanic origin, suggesting that the dissolution of the original shell components was mainly favored by the low P concentration in the paleolakes.

8. The volcanic influence compared between formations

As mentioned before, part of the LRF and the AZF stratigraphic record shows evidence of nearby volcanic activity. The LRF includes several ash fall layers throughout its section, particularly in cycle 4 (Figs. 2A, 5A) (Mancuso and Caselli, 2012), and the AZF presents lava flow levels in the lower section and ash fall levels in the upper section (Figs. 2B, 5B) (Ottone *et al*., 2011; Pedernera *et al*., 2019). Therefore, the LRF was located much farther from the volcanic center than the AZF (Fig. 8).

From a preservation point of view, the volcanic deposits show the lowest preservation of original shell components linked with basalt lava levels and ash fall levels. Notably, the AZF peperitic levels, which represent the interaction between lava and sediments, suggest a low temperature of the basalts, not able to significantly affect the lake bottom sediments (Ottone *et al*., 2011). Therefore, the possible thermal alteration of these lava flows

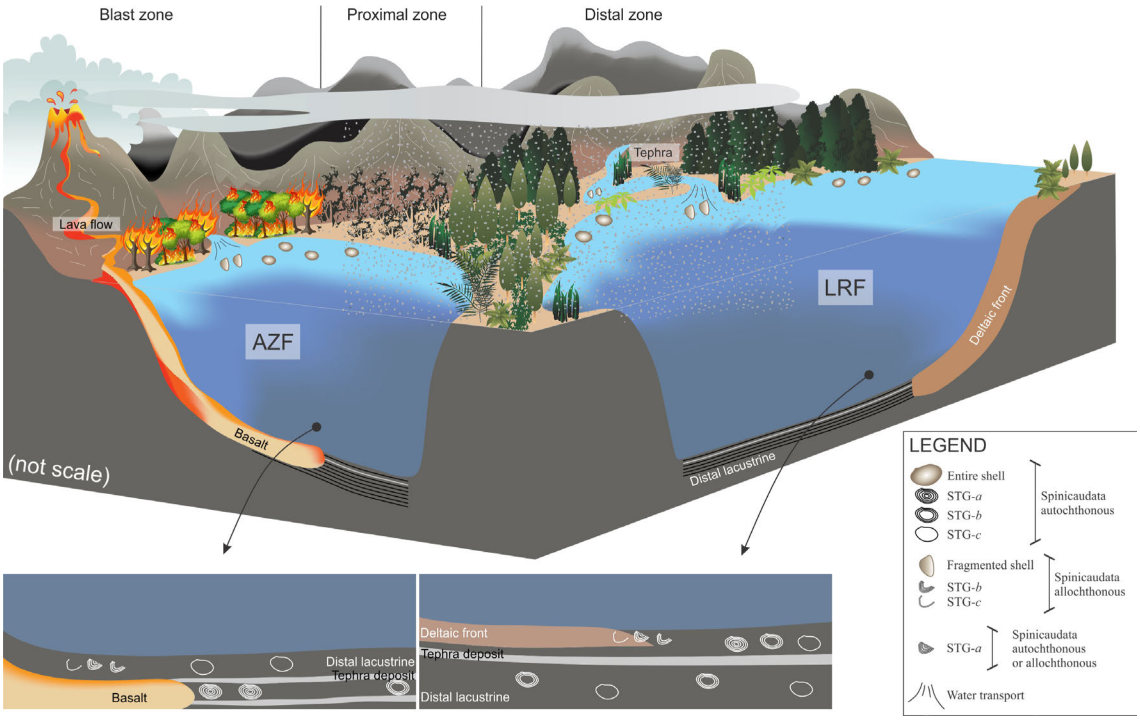

FIG. 8. Non-scaled representation of the effect of volcanic activity on terrestrial ecosystems and paleolakes at the Los Rastros Formation and Agua de la Zorra Formation. The diagram shows the location of the autochthonous/allochthonous spinicaudatan samples and the type of preservation, taking into account the second classification of taphonomic grades (STG).

can preliminarily be discarded. The alteration of the paleolake water due to volcanic activity and their microenvironmental diagenetic conditions can be explained mainly by pH modification (Jiang *et al*. 2011, 2012; Fürsich and Pan, 2015). Probably the acidic conditions favored by ash fall and lava flow input in the paleolakes enhanced the exchange of the main components of the shell (Ca and P) for those of the altered substrate (Holdaway and Clayton, 1982; Loope and Watkins, 1989; Butts and Briggs, 2011; Jiang *et al*., 2011, 2012). The opposite was reported for some plant remains from the AZF, where the volcanic deposits enhanced the preservation of the original organic components possibly due to the increase of sediment supply, carrying the plant remains to the active taphonomic zone, and/or affecting the microenvironmental conditions favoring plant preservation by diagenetic processes (Pedernera *et al*., 2020). However, the diagenetic conditions that favor the preservation of plant or shell remains are different. While low pH conditions favor the preservation of plant remains, the shells undergo the dissolution of their original components (Holdaway and Clayton, 1982; Loope and Watkins, 1989; Butts and Briggs, 2011; Fürsich and Pan, 2015). The influx of volcanic material can also increase the dissolved silica in paleolake waters, allowing the replacement of the original shell components by Si under specific microenvironmental diagenetic conditions.

From an ecological point of view, the LRF ash fall levels recorded in cycles 1, 2, and 4 show a lower taxa diversity and abundance (Fig. 2A) with a clear dominance of autochthonous specimens (Fig. 5A). In the AZF, the ash fall levels are recorded in the upper section, where the lower taxa richness and abundance are observed for this unit. In contrast, the AZF basalt lava levels recorded in the lower section show the highest abundance and richness (Fig. 2B) with a dominance of autochthonous specimens (Fig. 5B). Therefore, we suggest the ash fall levels in both paleolakes increased the depositional rates, the turbidity and the pH, disrupting the aquatic ecosystem. The increased level of densely packed shells of both units seems to be unrelated to this volcanic material influx. In contrast, the lava flows in the AZF enriched the aquatic ecosystem through the addition of dissolved moving elements and other nutrients. Moreover, the increase of densely packed multi-taxa levels between basalt lava levels supports recurrent paleolimnological changes in the AZF (Fig. 2B). Considering that spinicaudata assemblages are r-strategists, we assume that survival in these two paleoenvironments was favored through the resilience of their eggs, which hatched when paleolimnological conditions became favorable.

9. Conclusions

This study recognizes four new spinicaudata genera for the Los Rastros Formation (LRF) and three for the Agua de la Zorra Formation (AZF), in central-western Argentina. *Euestheria* is the most abundant genus in both formations, with the most extensive stratigraphic distribution, followed by *Triasoglypta*. The first level classification of the taphonomic grades (TG) allowed the characterization of the autochthonous and allochthonous spinicaudata assemblages in the LRF and AZF paleolakes. The second level taphonomic grade (STG), together with chemical analyses, allowed to relate the loss of morphological characters with the time of exposure of the shell in the water-sediment interface and the dissolution of the original chemical components of the shell (Ca and P). Both paleolakes contained P-poor water; however, the concentration of P in the LRF paleolake is higher than that of the AZF. The interaction of the surrounding and continuous volcanic activity with both paleolakes modified the environmental conditions necessary for developing spinicaudata assemblages and disfavored the preservation of the main chemical components of the shell. In turn, the significant increase of silica in the AZF paleolake, likely due to the surrounding volcanic activity, allowed the replacement of the original components of the shells by Si, and a better preservation of the morphological characters. In addition, the ash falls disturbed both the aquatic ecosystems of the paleolakes and the upstream section of the fluvial system. From a paleoecological perspective, the opportunistic (r-strategist) character of the spinicaudata is related to the paleolimnological modifications of the paleolakes of both formations.

Acknowledgments

We gratefully acknowledge T. Pedernera, C. Sancho, and M. Bourguet for their suggestions and assistance in the field; M. Bourguet for assistance in handling samples; S. Lassa for microphotography (LabMEB-IANIGLA-CONICET Mza). We would like to thank V. Vargas and L. Gachón (Secretaría de Cultura de La Rioja) for access to collections and working areas, we also thank, Administración de Parques Nacionales particularly and the staff of Parque Nacional Talampaya. Field research was supported by the PICT 2013-0805 (A. Mancuso) and PICT 2017-2159 (M. de la Fuente). Additional financial support was provided by the Consejo Nacional de Investigaciones Científicas y Técnicas (CONICET).

The Editor thanks S. Martínez and one anonymous reviewer for their assistance in evaluating this paper.

References

Allison, P.A. 1988. Phosphatized soft-bodied squids from the Jurassic Oxford Clay. Lethaia 21: 403e410. doi: 10.1111/j.1502-3931.1988.tb01769.x

Astrop, T.I. 2014. The evolutionary dynamics of sexual systems in deep time: an integrated biological and paleontological approach. Ph.D. Thesis (Unpublished) University of Akron: 233 p.

Astrop, T.I.; Hegna, T.A. 2015. Phylogenetic relationships between living and fossil spinicaudatan taxa (Branchiopoda Spinicaudata): reconsidering the evidence. Journal of Crustacean Biology 35 (3): 339-354.

Astrop, T.I.; Park, L.E.; Brown, B.; Weeks, S.C. 2012. Sexual discrimination at work: Spinicaudatan 'Clam Shrimp' (Crustacea: Branchiopoda) as a model organism for the study of sexual system evolution. Palaeontologia Electronica 15 (2): 1-15.

Astrop, T.I.; Sahni, V.; Blackledge, T.A.; Stark, A.Y. 2015. Mechanical properties of the chitin-calcium-phosphate "clam shrimp" carapace (Branchiopoda: Spinicaudata): implications for taphonomy and fossilization. Journal of Crustacean Biology 35 (2): 123-131.

Bachmann, G.H.; Kozur, H.W. 2004. The Germanic Triassic: correlations with the international scale, numerical ages and Milankovitch cyclicity. Hallesches. Jahrbuch für Geowissenschaften. Reihe B: Geologie. Paläontologie Mineralogie 26: 17-62.

Baird, W. 1862. Description of several new species of crustaceans, belonging to the genera *Estheria* and *Limnetis*. Proceedings of the Zoological Society of London 3 (1): 147-149.

Barker, P.; Telford, R.; Merdaci, O.; Williamson, D.; Taieb, M.; Vincens, A.; Gibert, E. 2000. The sensitivity of a Tanzanian crater lake to catastropheic tephra input and four millennia of climate change. The Holocene 10 (3): 303-310.

Behrensmeyer, A.K. 1991. Terrestrial vertebrate accumulations. *In* Taphonomy: releasing the data locked in the fossil record (Allison, P.A.; Briggs, D.E.G.; editors) Plenum: 291-335. New York.

Behrensmeyer, A.K.; Kidwell, S.M. 1985. Taphonomy's contributions to paleobiology. Paleobiology 11 (1): 105-119.

Behrensmeyer, A.K.; Hook, R.W. 1992. Paleoenvironmental contexts and taphonomic modes. *In* The Evolutionary Paleoecology of Terrestrial Plants and Animals (Behrensmeyer, A.K.; Damuth, J.D.; DiMichele, W.A.; Potts, R.; Sues, H.D.; Wing, S.L.; editors). University of Chicago Press: 15-136.

Behrensmeyer, A.K.; Kidwell, S.M.; Gastaldo, R.A. 2000. Taphonomy and paleobiology. Paleobiology 26 (S4): 103-147.

Benavente, C.A.; D'Angelo, J.A.; Crespo, E.M.; Mancuso, A.C. 2014. Chemometric approach to charophyte preservation (Triassic Cerro Puntudo Formation, Argentina): Paleolimnologic implications. Palaios 29 (9): 449-459.

Benavente, C.A.; Mancuso, A.C.; Irmis, R.B.; Bohacs, K.M.; Matheos, S. 2021. Tectonically conditioned record of continental interior paleoclimate during the Carnian Pluvial Episode: The Upper Triassic Los Rastros Formation, Argentina. Geological Society of America Bulletin 134 (1-2): 60-80.

Benvenuto, C.; Knott, B.; Weeks, S.C. 2009. Mate-guarding behavior in clam shrimp: a field approach. Behavioral Ecology 20 (5): 1125-1132.

Berner, R.A. 1968. Calcium carbonate concretions formed by the decomposition of organic matter. Science 159: 195-197.

Bishop, J.A. 1967. Seasonal occurrence of a branchiopod crustacean, Limnadia stanleyana King (Conchostraca) in eastern Australia. The Journal of Animal Ecology 36: 77-95.

Brea, M.; Artabe, A.E. 1999. Apocalamitaceae (Sphenophyta) triásicas de la Formación Paramillo, Agua de la Zorra, provincia de Mendoza, Argentina. Ameghiniana 36: 389-400.

Brett, C.E.; Baird, G.C. 1986. Comparative taphonomy: a key to paleoenvironmental interpretation based on fossil preservation. Palaios 1: 207-227.

Briggs, D.E. 2003. The role of decay and mineralization in the preservation of soft-bodied fossils. Annual Review of Earth and Planetary Sciences 31 (1): 275-301.

Bustos Escalona, E.L. 2020. Paleoecología y Tafonomía de Artrópodos en secuencias fluvio-lacustres triásicas del Oeste de Argentina. Tesis Doctoral (Inédito), Universidad Nacional de San Luis: 263 p.

Bustos Escalona, E.L.; Mancuso, A.C.; Benavente, C.A.; Arcucci, A.B. 2017. Análisis tafonómico de Spinicaudata ("Conchostraca", Crustacea) en la Formación Los Rastros (Triásico Superior) Cuenca Ischigualasto-Villa Unión, La Rioja, Argentina. *In* Reunión de comunicaciones de la Asociación Paleontológica Argentina, Resúmenes: 18-19.

Bustos Escalona, E.L.; Mancuso, A.C.; Benavente, C.A. 2019. Bioerosion on Spinicaudata shells from a Triassic freshwater paleolake, Mendoza, Argentina. Palaios 34 (12): 616-630. doi: https://doi.org/10.2110/palo.2019.044

Butts, S.H.; Briggs, D.E.G. 2011. Silicification through time. *In* Taphonomy: Process and Bias Through Time (Allison, P.A.; Bottjer, D.J.; editors). Topics in Geobiology 32: Springer 411: 34 p. Dordrecht.

Cáceres, C.E.; Tessier, A.J. 2003. How long to rest: the ecology of optimal dormancy and environmental constraint. Ecology 84 (5): 1189-1198.

Chen, P.J.; Hudson, J.D. 1991. The Conchostracan Fauna of the Great Estuarine Group, Middle Jurassic, Scotland. Palaeontology 34 (3): 515-545.

Cohen, A.S. 2003. Paleolimnology: History and Evolution of Lake Systems. Oxford University Press: 350 p. Oxford.

Dale, V.H.; Swanson, F.J.; Crisafulli, C.M. 2005. Disturbance, survival, and succession: understanding ecological responses to the 1980 eruption of Mount St. Helens. *In* Ecological Responses to the 1980 Eruption of Mount St. Helens (Dale, V.H.; Swanson, F.J.; Crisafulli, C.M.; editors). Springer: 3-11. New York.

Driscoll, E.G. 1970. Selective bivalve shell destruction in marine environments; a field study. Journal of Sedimentary Research 40 (3): 898-905.

Driscoll, E.G.; Weltin, T.P. 1973. Sedimentary parameters as factors in abrasive shell reduction. Palaeogeography, Palaeoclimatology, Palaeoecology 13 (4): 275-288.

Dumont, H.J.; Negrea, S.V. 2002. Guides to the identification of the microcrustaceans of the continental waters of the world: Branchiopoda. Backhyus: 398 p.

Farinati, E.; Zavala, C. 1995. Análisis tafonómico de moluscos y análisis de facies en la serie holocena del río Quequén Salado, provincia de Buenos Aires, Argentina. *In* Congreso Argentino de Paleontología y Bioestratigrafía, No. 6: 117-122. Trelew.

Fernández-López, S.R. 2000. Temas de Tafonornía, Departamento de Paleontología. Universidad Complutense de Madrid: 167 p.

Ferreira-Olivera, L.G. 2007. “Conchostráceos permianos da Bacia do Paraná: taxonomia, evolução, bioestratigrafia e paleobiogeografia”. Tesis Doctoral (Inédito), Universidade Estadual Paulista: 185 p.

Fryer, G.; 1996. Diapause, a potent force in the evolution of freshwater crustaceans. Hydrobiologia 320 (1): 1-14.

Fürsich, F.; Pan, Y. 2015. Diagenesis of bivalves from Jurassic and Lower Cretaceous lacustrine deposits of northeastern China. Geological Magazine 153 (1): 17-37.

Fürsich, F.T.; Pan, Y.H.; Wang, Y.Q. 2016. Biostratinomy of bivalves from Jurassic and Early Cretaceous lakes of NE China. Palaeoworld 25 (3): 399-405. doi: https://doi.org/10.1016/j.palwor.2015.11.001

Gabbott, S.E. 1998. Taphonomy of the Ordovician Soom Shale Lagerstätte: an example of soft tissue preservation in clay minerals. Palaeontology 41 (4): 631-667.

Gallego, O.F. 1992. Conchostracos triásicos de Mendoza y San Juan, Argentina. Ameghiniana 29 (2): 159-175.

Gallego, O.F. 1996. Revisión de algunos conchostracos de la Formación Santa María (Triásico Medio a Superior) del Estado de Río Grande del Sur (Brasil). Acta Geologica Leopoldensia 19 (43): 59-76.

Gallego, O.F. 1999a. *Tryasoglypta santamariensis* Gallego nov. comb. (Conchostraca) de la Formación Santa María (Triásico Medio-Superior) de Brasil. Geociências 4: 61-66.

Gallego, O.F. 1999b. Estudio sistemático de las faunas de conchóstracos triásicos de la República Argentina. Tesis Doctoral (Inédito), Universidad Nacional de Córdoba, Facultad de Ciencias Exactas, Físicas y Naturales: 210 p.

Gallego, O.F. 2001. Conchostracofauna sudamericana del Paleozoico y Mesozoico: estado actual del conocimiento. Parte I: Argentina y Chile. Acta Geológica Leopoldensia 24 (52-53): 311-328.

Gallego, O.F. 2005. First record of the family Palaeolimnadiopseidae Defretín–LeFranc, 1965 (Crustacea-Conchostraca) in the Triassic of Argentina. Journal of South American Earth Sciences 18 (2): 223-231.

Gallego, O.F. 2010. A new crustacean clam shrimp (Spinicaudata: Eosestheriidae) from the Upper Triassic of Argentina and its importance for ‘Conchostracan’ taxonomy. Alcheringa 34 (2): 179-195.

Gallego, O.F.; Melchor, R.N. 2000. La Familia Ulugkemidae Novozhilov, 1958 (Conchostraca) en el Triásico de Argentina: implicancias paleobiogeográficas. Ameghiniana 37 (1): 47-51.

Gallego, O.F.; Martins-Neto, R.G. 2005. A preliminary approach to stratigraphical distribution of the Triassic insect and conchostracan faunas from southern South America. *In* Abstracts Gondwana (Pankhurst, R.J.; Veiga, G.D.; editors), No. 12, Resúmenes: p. 164. Mendoza

Gallego, O.F.; Martins-Neto, R.G.; 2006. Propuesta preliminar sobre la distribución estratigráfica de las faunas triásicas de insectos y conchostracos de Argentina, Chile y sur de Brasil. Comunicaciones Científicas y Tecnológicas, Universidad Nacional del Nordeste, Resumen: B-009. Corrientes.

Gallego, O.F.; Martins-Neto, R.G.; Carmona, M.J. 2001. Nuevos registros de artrópodos (Insecta y Conchostraca) en el Triásico de la Argentina: comentarios sobre su afinidad con faunas de Laurasia y Gondwana. Reunión de Comunicaciones Científicas y Tecnológicas, Universidad Nacional del Nordeste Resumen: B-057. Corrientes.

Gallego, O.F.; Zavattieri, A.M.; López-Arbarello, A. 2004. Conchóstracos y restos de peces de la localidad tipo de la Formación Río Mendoza (Triásico Medio), Provincia de Mendoza, Argentina. Ameghiniana 41 (3): 289-301.

Gallego, O.F.; Crisafulli, A.; Gnaedinger, S.C.; Adami-Rodrígues, K.; Martins-Neto, R.G.; Lara, M.B.; Monferran, M.D. 2008. Análisis preliminar del registro y la biodiversidad de los invertebrados continentales y de la paleoflora de Argentina y Brasil durante la transición Pérmico-Triásico. Comunicaciones Científicas y Tecnológicas. Secretaría General de Ciencia y Técnica, Universidad Nacional del Nordeste. Corrientes

Ghosh, S.C. 1980. SEM observation on spined fossil conchostracan: EUREM 80: Electron Microscopy. *In* European Congress on Electron Microscopy, No 7: 482-483. Netherlands

Ghosh, S.C. 1984. Microcrystal of evaporites and Gondwana palaeogeography. *In* European Electronic Microscopy Congress, No. 8: 1055-1056. Budapest.

Ghosh, S.C. 2011. Estheriids (fossil conchostraca) of Indian Gondwana. Palaeontologia Indica 54: 1-146.

Ghosh, S.C.; Dutta, A. 1996. A critical review of fossil Conchostraca of Permian-Triassic periods. *In* Gondwana Nine. Ninth International Gondwana Symposium, No. 27: 73-88. India.

Ghosh, S.C.; Dutta, A.; Nandi, A.; Mukhopadhaya, S. 1987a. Estheriid zonation in the Gondwana. The Palaeobotanist 36: 143-153.

Ghosh, S.C.; Bhattacharji, T.K.; Dutta, A.; Sen, C.R.; Dutta, N.R. 1987b. A note on the biostratigraphy of Panchet Formation around Andal Area, Eastern part of Raniganj Coalfield, West Bengal. Geological Society of India Special Publications 11: 233-241.

Gislén, T.R.E. 1937. Contributions to the ecology of Limnadia. Acta Universitatis Lundensis 32: 1-20.

Golubic, S.; Schneider, J. 1979, Carbonate Dissolution. *In* Studies in Environmental Science (Trudinger, P.A.; Swaine, D.J.; editors). Elsevier 3: 107-129.

Gore, P.J.W. 1988. Lacustrine sequences in an early Mesozoic rift basin: Culpeper Basin, Virginia, USA. Geological Society, London, Special Publications 40 (1): 247-278.

Gulbrandsen, R. 1969. Physical and chemical factors in the formation of marine apatite. Economic Geology 64 (4): 365-382. doi: https://doi.org/10.2113/gsecongeo.64.4.365

Harrington, H.J. 1971. Descripción geológica de la hoja 22c," Ramblón" Provincias de Mendoza y San Juan. Dirección Nacional de Geología y Minería, Boletín 114: 93 p.

Hegna, T.A.; Czaja, A.D.; Rogers, D.C. 2020. Raman spectroscopic analysis of the composition of the clam-shrimp carapace (Branchiopoda: Laevicaudata, Spinicaudata, Cyclestherida): a dual calcium phosphate-calcium carbonate composition. The Journal of Crustacean Biology 40 (6): 756-760.

Hethke, M.; Fürsich, F.T.; Jiang, B.Y.; Pan, Y.H. 2013. Seasonal to sub-seasonal palaeoenvironmental changes in Lake Sihetun (Lower Cretaceous Yixian Formation, NE China). International Journal of Earth Sciences 102 (1): 351-378.

Holdaway, H.K.; Clayton, C.J. 1982. Preservation of shell microstructure in silicified brachiopods from the Upper Cretaceous Wilmington Sands of Devon. Geological Magazine 119: 371-382.

Horne, F.R. 1967. Effects of physical and chemical factors on the distribution and occurrence of some southeastern Wyoming phyllopods. Ecology 48 (3): 472-477.

Hu, L.; Zhao T.; Pan, Y. 2020. Spinicaudatans from the Yixian Formation (Lower Cretaceous) and the Daohugou Beds (Jurassic) of Western Liaoning, China. Cretaceous Research 105: 104073.

Jenisch, A.G.; Lehn, I.; Gallego, O.F.; Monferran, M.D.; Horodyski, R.S.; Faccini, U.F. 2017. Stratigraphic distribution, taphonomy and paleoenvironments of Spinicaudata in the Triassic and Jurassic of the Paraná Basin. Journal of South American Earth Sciences 80: 569-588.

Jiang, B.Y.; Fürsich, F.T.; Sha, J.G.; Wang, B.; Niu, Y.Z. 2011. Early Cretaceous volcanism and its impact on fossil preservation in Western Liaoning, NE China. Palaeogeography, Palaeoclimatology, Palaeoecology 302: 255-69.

Jiang, B.Y.; Fürsich, F.T.; Hethke, M. 2012. Depositional evolution of the Early Cretaceous Sihetun Lake and implications for regional climatic and volcanic history in western Liaoning, NE China. Sedimentary Geology 257-260: 31-44.

Kapler, O. 1960. Aus dem Leben der *Leptestheria dahalacensis* RÜPPEL. Casopis Slezského Musea 9: 101-110.

Karr, J.A.; Clapham, M.E. 2015. Taphonomic biases in the insect fossil record: shifts in articulation over geologic time. Paleobiology 41 (1): 16-32.

Klug, C.; Hagdorn, H.; Montenari, M. 2005. Phosphatized soft-tissue in Triassic bivalves. Palaeontology 48: 833-852. doi: https://doi.org/10.1111/j.1475-4983.2005.00485.x

Klunzinger, F. 1864. Beiträge zur Kenntnis der Limadiden. Zeitschrift für Wissenschaftliche Zoologie 14: 139-164.

Kobayashi, T. 1975. Upper Triassic estheriids in Thailand and the conchostracan development in Asia in the Mesozoic Era. Geology and Palaeontology of Southeast Asia 16: 57-90.

Kokogian, D.A.; Boggetti, D.A. 1987. Reconocimiento de las formaciones Barrancas y Punta de las Bardas en la zona de Paramillos de Uspallata, prov. Mendoza, Argentina. *In* Congreso Geológico Argentino, No 10, Acta 3: 131-134. San Miguel de Tucumán.

Kokogian, D.A.; Mancilla, O. 1989. Análisis estratigráfico secuencial de la Cuenca Cuyana. Cuencas Sedimentarias Argentinas 6: 169-201.

Konhauser, K.O.; Phoenix, V.R.; Bottrell, S.H.; Adams, D.G.; Head, I.M. 2001. Microbial-silica interactions in Icelandic hot spring sinter: possible analogues for some Precambrian siliceous stromatolites. Sedimentology 48 (2): 415-433.

Kozur, H.W. 1993. Range charts of Conchostracans in the Germanic Buntsandstein. *In* The Nonmarine Triassic. (Lucas, S.G.; Morales, M.; editors) New Mexico Museum of Natural History and Science Bulletin 3: 249-253.

Kozur, H.W.; Seidel, G. 1983a. Revision der Conchostracen-Faunen des unteren und mittleren Buntsandsteins Teil I. Zeischriftfür Geologische Wissenschaften 11: 289-417.

Kozur, H.W.; Seidel, G. 1983b. Die Biostratigraphie des unteren und mittleren Buntsandsteins unter besonderer Berücksichtigung der Conchostracen. Zeitschrift für Geologische Wissenschaften 11: 429-464.

Kozur, H.W.; Weems, R.E. 2007. Upper Triassic conchostracan biostratigraphy of the continental basins of eastern North America: its importance for correlating Newark Supergroup events with the Germanic Basin and the International Geologic Time Scale. *In* The Global Triassic (Lucas, S.G.; Spielmann, J.A.; editors) New Mexico Museum of Natural History and Science Bulletin 41: 137-188.

Kozur, H.W.; Weems, R.E. 2010. The biostratigraphic importance of conchostracans in the continental Triassic of the northern hemisphere. *In* The Triassic Timescale (Lucas, S.G.; editor). Geological Society Special Publications 334: 351-417. London.

Krishnan, G. 1958. Some aspects of cuticular organization of the branchiopod, Streptocephalus dichotomus. Quarterly Journal of Microscopical Science 3 (47): 359-371.

Linares, E. 2007. Catálogo de edades radimétricas de la República Argentina, Años 1957-2005. Asociación Geológica Argentina, Serie "F": CD-2. Buenos Aires.

Lipman, P.W.; Mullineaux, D.R. 1982. The 1980 eruptions of Mount St. Helens, Washington. US Government Printing Office No. 12550: 844 p.

Lockley, M.G.; Rice, A. 1990. Volcanism and fossil biotas. Geological Society of America: 126 p.

Loope, D.B.; Watkins, D.K. 1989. Pennsylvanian fossils replaced by red chert; early oxidation of pyritic precursors. Journal of Sedimentary Research 59 (3): 375-386.

Lovecchio, J.P.; Rohais, S.; Joseph, P.; Bolatti, N.D.; Ramos, V.A. 2020. Mesozoic rifting evolution of SW Gondwana: A poly-phased, subduction-related, extensional history responsible for basin formation along the Argentinean Atlantic margin. Earth-Science 203: 1-27.

Mancuso, A.C. 2005. Tafonomía en ambientes lacustres: estudio integral de las asociaciones fósiles de las secuencias lacustres del Triásico Medio de la Cuenca de Ischigualasto-Villa Unión (formaciones Chañares, Los Rastros e Ischichuca). Tesis Doctoral (Inédito). Universidad de Buenos Aires: 208 p. Buenos Aires.

Mancuso, A.C.; Gallego, O.F. 2000. Primer análisis tafonómico de una asociación de invertebrados fósil registrada en la Formación Los Rastros (Triásico Medio, Argentina). Ameghiniana Suplemento Resúmenes 37: 41R.

Mancuso, A.C.; Marsicano, C.A. 2008. Paleoenvironments and taphonomy of a Triassic lacustrine system (Los Rastros Formation, central-western Argentina). Palaios 23 (8): 535-547.

Mancuso, A.C.; Caselli, A.T. 2012. Paleolimnology evolution in rift basins: the Ischigualasto-Villa Unión Basin (central-western Argentina) during the Triassic. Sedimentary Geology 275: 38-54.

Mancuso, A.C.; Chemale, F.; Barredo, S.; Ávila, J.N.; Ottone, E.G.; Marsicano, C. 2010. Age constraints for the northernmost outcrops of the Triassic Cuyana Basin, Argentina. Journal of South American Earth Sciences 30 (2): 97-103.

Mancuso, A.C.; Krapovickas, V.; Benavente, C.A.; Marsicano, C.A. 2020. An integrative physical, mineralogical and ichnological approach to characterize underfilled lake-basins. Sedimentology 67 (6): 3088-3118.

Martínez, R.N.; Sereno, P.C.; Alcober, O.A.; Colombi, C.E.; Renne, P.R.; Montañez, I.P.; Currie, B.S. 2011. A basal dinosaur from the dawn of the dinosaur era in southwestern Pangaea. Science 331 (6014): 206-210.

Massabie, A.H.; Rapalini, A.E.; Soto, J.L. 1986. Estratigrafía del Cerro Los Colorados, Paramillo de Uspallata, Mendoza. *In* Jornadas sobre Geología de Precordillera, No. 1, Resúmenes 1: 71-76. San Juan.

Massaferro, J.; Correa-Metrio, A.; De Oca, F.M.; Mauad, M. 2018. Contrasting responses of lake ecosystems to environmental disturbance: a paleoecological perspective from northern Patagonia (Argentina). Hydrobiologia 816 (1): 79-89.

Massal, L. 1954. Deuxième note sur le milieu et la croissance des Esthérias. Bulletin de la Société des Sciences Naturelles de Tunisie 7: 163-181.

McKenzie, J.A. 1981. Holocene dolomitization of calcium carbonate sediments from the coastal sabkhas of Abu Dhabi, UAE: a stable isotope study. The Journal of Geology 89 (2): 185-198.

McNamara, M.E.; Orr, P.J.; Manzocchi, T.; Alcalá, L.; Anadón, P.; Peñalver, E. 2011. Biological controls upon the physical taphonomy of exceptionally preserved salamanders from the Miocene of Rubielos de Mora, northeast Spain. Lethaia 45 (2): 210-226.

McNamara, M.E.; Orr, P.J.; Alcalá, L.; Anadón, P.; Peñalver, E. 2012. What controls the taphonomy of exceptionally preserved taxa: Environment or biology? A case study using frogs from the Miocene Libros Konservat-Lagerstätte (Teruel, Spain). Palaios 27 (2): 63-77.

Monferran, M.D.; D'Angelo, J.A.; Cabaleri, N.G.; Gallego, O.F.; Garban, G. 2018. Chemical taphonomy and preservation modes of Jurassic spinicaudatans from Patagonia: a chemometric approach. Journal of Paleontology 92 (6): 1054-1065.

Moore, W.G. 1965. New distribution records for Conchostraca (Crustacea, Branchiopoda), with an account of their occurrence in Louisiana. *In* Proceedings of the National Academy of Sciences 28: 41-44.

Moore, W.G.; Burn, A. 1968. Lethal oxygen thresholds for certain temporary pond invertebrates and their applicability to field situations. Ecology 49 (2): 349-351.

Novojilov, N.I. 1970. Vymmershie Lomnadioidei (Conchostraca-Limnadioidea). Nauka: 238 p. Moscow.

Okorafor, K.A. 2011. Ecological responses of freshwater components to climate change impacts: A review. ARPN Journal of Science and Technology 4 (11): 654-665.

Olempska, E. 2004. Late Triassic spinicaudatan crustaceans from southwestern Poland. Acta Palaeontologica Polonica 49 (3): 429-442.

Orr, P.J.; Briggs, D.E.G. 1999. Exceptionally preserved conchostracans and other crustaceans from the Upper Carboniferous of Ireland. Palaeontology, Special Papers 62: 5-68.

Orr, P.J.; Kearns, S.L.; Briggs, D.E.G. 2002. Backscattered Electron Imaging of Fossils Exceptionally-Preserved as Organic Compressions. Palaios 17 (1): 110-117.

Orr, P.J.; Briggs, D.E.G.; Kearns, S.L. 2008. Taphonomy of Exceptionally Preserved Crustaceans from the Upper Carboniferous of Southeastern Ireland. Palaios 23 (4): 298-312.

Ottone, E.G.; Avellaneda, D.; Koukharsky, M. 2011. Plantas triásicas y su relación con el volcanismo en la Formación Agua de la Zorra, provincia de Mendoza, Argentina. Ameghiniana 48 (2): 177-188.

Pan, Y.; Sha, J.; Fürsich, F.T.; Wang, Y.; Zhang, X.; Yao, X. 2011. Dynamics of the lacustrine fauna from the Early Cretaceous Yixian Formation, China: implications of volcanic and climatic factors. Lethaia 45 (3): 299-314. doi: https://doi.org/10.1111/j.1502-3931.2011.00284.x

Payne, R.J.; Egan, J. 2017. Using palaeoecological techniques to understand the impacts of past volcanic eruptions. Quaternary international 499: 278-289.

Pedernera, T.E. 2020. Tafonomía de las paleofloras triásicas del centro-oeste de la Argentina. Tesis Doctoral (Inédito). Universidad de Buenos Aires: 285 p. Buenos Aires.

Pedernera, T.E.; Ottone, E.G.; Mancuso, A.C.; Benavente, C.A.; Abarzúa, F. 2019. Tafoflora sin-eruptiva de la Formación Agua de la Zorra (Triásico Superior) Cuenca Cuyana, Mendoza, Argentina. Andean Geology 46 (3): 604-628. doi: http://dx.doi.org/10.5027/andgeoV46n3-3228

Pedernera, T.E.; Mancuso, A.C.; Benavente, C.A.; Ottone, E.G. 2020. Plant taphonomy in a lake affected by volcanism (agua de la Zorra Formation, Upper Triassic) Mendoza, Argentina. Palaios 35 (6): 245-261. doi: https://doi.org/10.2110/palo.2019.104

Pedernera, T.E.; Mancuso, A.C.; Ottone, E.G. 2021. The influence of volcanic activity and trophic state on plant taphonomic processes in Triassic lacustrine-deltaic systems of western Gondwana. Lethaia 54 (4): 521-539. doi: https://doi.org/10.1111/let.12420

Petr, T. 1968. Population changes in aquatic invertebrates living on two water plants in a tropical man-made lake. Hydrobiologia 32 (3): 449-485.

Plotnick, R.E. 1986. Taphonomy of a modern shrimp; implicaions for the arthropod fossil record. Palaios 1: 286-293.

Prámparo, M.B.; Ballent, S.C.; Gallego, O.F.; Milana, J.P. 2005. Paleontología de la Formación Lagarcito (Cretácico inferior) en la provincia de San Juan, Argentina. Ameghiniana 42 (1): 93-114.

Ramos, V.A.; Kay, S.M. 1991. Triassic rifting and associated basalts in the Cuyo basin, central Argentina. En Andean magmatism and its tectonic setting. Geological Society of America Boulder 265: 79-91.

Renaut, R.W.; Jones, B.; Tiercelin, J.J.; Tarits, C. 2002. Sublacustrine precipitation of hydrothermal silica in rift lakes: Eidence from Lake Baringo, central Kenya Rift Valley. Sedimentary Geology 148 (1-2): 235-257.

Renaut, R.W.; Owen, R.B.; Jones, B.; Tiercelin, J.J.; Tarits, C.; Ego, J.K.; Konhauser, K.O. 2012. Impact of lake-level changes on the formation of thermogene travertine in continental rifts: evidence from Lake Bogoria, Kenya Rift Valley. Sedimentology 60 (2): 428-468.

Rieder, N.; Abaffy, P.; Hauf, A.; Lindel, M.; Weishäupl, H. 1984. Funktionsmorphologische Untersuchungen an den Conchostracen *Leptestheria dahalacensis* und *Limnadia lenticularis* (Crustacea, Phyllopoda, Conchostraca). Zoologische Beiträge 28 (3): 417-444.

Royan, J.P. 1976. Studies on the gut contents of *Leptestheriella maduraiensis* (Conchostraca: Branchiopoda) Nayar and Nair. Hydrobiologia 51 (3): 209-212.

Rzoska, J. 1961. Observation on tropical rainpools and general remarks on temporary waters. Hidrobiologia 17 (4): 265-286.

Schindler, D.W. 1977. Evolution of phosphorus limitation in lakes. Science 195 (4275): 260-262.

Seilacher, A.; Reif, W.E.; Westphal, F. 1985. Sedimentological, ecological and temporal patterns of fossil Lagerstätten. Philosophical Transactions of the Royal Society of London. Biological Sciences 311 (1148): 5-24.

Shen, Y.B.; Gallego, O.F.; Zavattieri, A.M. 2001. A new conchostracan genus from Triassic Potrerillos Formation, Argentina. Acta Geologica Leopoldensia 24: 227-236.

Smith, G.A. 1987. The influence of explosive volcanism on fluvial sedimentation: The Deschutes Formation (Neogene) in Central Oregon. Journal of Sedimentary Petrology 57 (4): 613-29.

Smith, D.M.; Moe-Hoffman, A.P. 2007. Taphonomy of Diptera in lacustrine environments: A case study from the Florissant Fossil Beds, Colorado. Palaios 22 (6): 623-629.

Spencer, B.; Hall, T.S.; 1896. Crustacea. *In* Report on the work of the Horn Scientific Expedition to central Australia. Part II. Zoology (Horn, W.A.; editor). Dulao and Company 1: 227-248.

Sterner, R.W. 2008. On the Phosphorus Limitation Paradigm for Lakes. International Review of Hydrobiology 93 (4-5): 433-445.

Stigall, A.L.; Hartman, J.H. 2008. A new spinicaudatan genus (Crustacea:'Conchostraca') from the Late Cretaceous of Madagascar. Palaeontology 51 (5): 1053-1067.

Stigall, A.L.; Babcock, L.E.; Briggs, D.E.; Leslie, S.A. 2008. Taphonomy of lacustrine interbeds in the Kirkpatrick Basalt (Jurassic), Antarctica. Palaios 23 (6): 344-355.

Stigall, A.L.; Hembree, D.I.; Gierlowski-Kordesch, E.H.; Weismiller, H.C. 2014. Evidence for a dioecious mating system in Early Jurassic *Hardapestheria maxwelli* gen. et sp. nov. (Crustacea, Branchiopoda, Spinicaudata) from the Kalkrand Formation of Namibia. Palaeontology 57 (1): 127-140.

Tasch, P. 1963. Paleolimnology, Part 3: Marion and Dickinson Counties, Kansas, with Additional Sections in Harvey and Sedgwick Counties: Stratigraphy and Biota. Journal of Paleontology 37: 1233-1251.

Tasch, P. 1969. Branchiopoda. Treatise on invertebrate paleontology, part R. Arthropoda 4: 128-192.

Tasch, P. 1987. Fossil Conchostraca of the Southern Hemisphere and continental drift: Paleontology, biostratigraphy, and dispersal. Geological Society of America 165: 289 p.

Tasch, P.; Zimmerman, J.R. 1961. Fossil and Living Conchostracan Distribution in Kansas-Oklahoma across a 2OO-Millon-Year Time Ga. Science 133 (3452): 584-586.

Tasch, P.; Shaffer, B.L. 1964. Conchostracans: living and fossil from Chihuahua and Sonora, Mexico. Science 143 (3608): 806-807.

Tassi, L.V. 2015. Estudio de la fauna de Spinicaudata a través del Triásico de Argentina y su recuperación luego del evento de extinción Permo-Triásica. Tesis Doctoral (Inédito). Universidad Nacional de Córdoba: 241 p.

Tassi, L.V.; Monti, M.; Gallego, O.F.; Zavattieri, A.M.; Lara, M.B. 2013. The first spinicaudatan (Crustacea-Diplostraca) from the Permo-Triassic continental sequences in South America and its paleoecological context. Alcheringa: An Australasian Journal of Palaeontology 37 (2): 189-201.

Tassi, L.V.; Zavattieri, A.M.; Gallego, O.F. 2015. Triassic spinicaudatan fauna from the Cerro de Las Cabras Formation (Cuyo Basin), Mendoza Province (Argentina): description of new species and revision of previous records. Ameghiniana 52 (23): 241-264.

Thiéry, A. 1996: Branchiopodes. 1. Ordres des Anostracés, Notostracés, Spinicaudata et Laevicaudata (Ostracoda Latreille, 1802). *In* Traité de Zoologie, Anatomie, Systématique, Biologie, Tome VII, Crustacés, Fascicule 2, (Forest, J.; editor). Généralités (suite) et Systématique: 287-351.

Uliana, M.A.; Biddle, K.T. 1988. Mesozoic-Cenozoic paleogeographic and geodynamic evolution of southern South America. Revista Brasileira de Geociencias 18 (2): 172-190.

Wang, B.; Zhang, H.; Jarzembowski, E.A.; Fang, Y.; Zheng, D. 2013. Taphonomic variability of fossil insects: a biostratinomic study of Palaeontinidae and Tettigarctidae (Insecta: Hemiptera) from the Jurassic Daohugou Lagerstätte. Palaios 28 (4): 233-242.

Warren, J.K. 1986. Shallow-water evaporitic environments and their source rock potential. Journal of Sedimentary Petrology 56: 442-454.

Webb, J.A. 1979. A reappraisal of the palaeoecology of conchostracans (Crustacea: Branchiopoda). Neues Jahrbuch für Geologie und Paläontologie Abhandlungen 158: 259-275.

Wedmann, S. 1998. Taphonomie der Bibionidae (Insecta: Diptera) aus der oberoligozänen Fossillagersta¨tte Enspel (Deutschland). Neues Jahrbuch für Geologie und Paläontologie Monatshefte 9: 513-528.

Weeks, S.C.; Zucker, N. 1999. Rates of inbreeding in the androdioecious Spinicaudatan Eulimnadia texana. Canadian Journal of Zoology 77: 1402-1408. doi: https://doi.org/10.1139/z99-103

Wetzel, R.G. 2001. Limnology: lake and river ecosystems (3º Ed.). Gulf professional publishing: 1006 p.

Wilson, M. 1988. Taphonomic processes: Information loss and information gain. Geoscience Canada 15 (2): 131-148.

Zhang, W.T.; Shen, Y.B.; Niu, S. 1990. Discovery of Jurassic conchostracans with well-preserved soft parts and notes on its biological significance. Palaeontologia Cathayana. Springer: 311-351.

Manuscript received: February 07, 2022; revised/accepted: July 20, 2023; available online: July 28, 2023.

Supplemental File

Statistical analyses

Two statistical analyses were performed to determine if there is a significant difference between the Taphonomic Grades (TG) identified in two different paleolakes. The analyses were performed using data collected during systematic sampling of the Los Rastros Formation (LRF) at the Gualo area and the Agua de la Zorra Formation (AZF) at the Paramillos de Uspallata area.

TABLE S1. DATA USED FOR THE CHI-SQUARE TEST.

Taphonimic Grades	LRF	AZF
1	1,275	973
2	225	676

Total number of spinicaudatans by taphonomic grade (**TG**). Los Rastros Formation (**LRF**); Agua de la Zorra Formation (**AZF**).

TABLE S2. DETAIL OF THE DIFFERENT TAPHONOMIC GRADES, AND THE PERCENTAGES OF OCCURRENCE FOR THE LOS RASTROS FORMATION, ISCHIGUALASTO-VILLA UNIÓN BASIN (CARNIANO, UPPER TRIASSIC) AND AGUA DE LA ZORRA FORMATION, CUYANA BASIN (MIDDLE-UPPER TRIASSIC)

Taphonomic classification	Nomination	Percentage (%)	
		LRF	AZF
TG	**1**	85	59
	2	15	41
STG	***a***	3	9
	b	49	36
	c	48	55

TG: Taphonomic Grades; **STG:** Second Level Taphonomic Grades; **LRF:** Los Rastros Formation; **AZF:** Agua de la Zorra Formation.

In the first instance, a resampling statistic was performed with the values of the number of specimens identified according to TG-1 and TG-2, and the calculated percentages of these in each formation (LRF and AZF) (Table S1; Table S2). To verify the results obtained with the resampling statistic, a Chi-square test was performed. Both analyses were carried out with R-Studio software.

1. Resampling statistic

Resampling is a statistical procedure that generates a large number of samples simulating a resampling of the original sample. For this statistic, the number of complete (TG-1) and fragmented (TG-2) shell specimens obtained in the systematic sampling in LRF and AZF (Table S1) was used as a base. For each formation, 10,000 resamplings were programmed. This statistic allowed us to simulate the number of TG-1 and TG-2 specimens that we would obtain if we performed successive random sampling. Table S3 shows the values of the frequency in which TG-1 specimens were obtained for LRF and AZF.

TABLE S3. DATA TABLE OF THE RESAMPLING RESULTS FOR THE SAMPLES ANALYZED FROM LOS RASTROS FORMATION (LRF) AND AGUA DE LA ZORRA FORMATION (AZF).

Measurements	Min.	1st Qu.	Median	Mean	3rd Qu.	Max.
LRF	80.8	84.3	85	85	85.8	88.6
AZF	51.9	57.9	59	58.98	60	64.8

For better visualization of the results, histogram graphs were made with the results obtained (Fig. S1). The resampling statistic for our sites indicates that TG-1 in AZF ranges from 51.9-64.8% with a mean frequency of 58.98%; while in LRF, TG-1 ranges from 80.8-88.6 % with a mean frequency of 85%. These results are in agreement with those obtained in the sequential sampling of both formations (see Table S2).

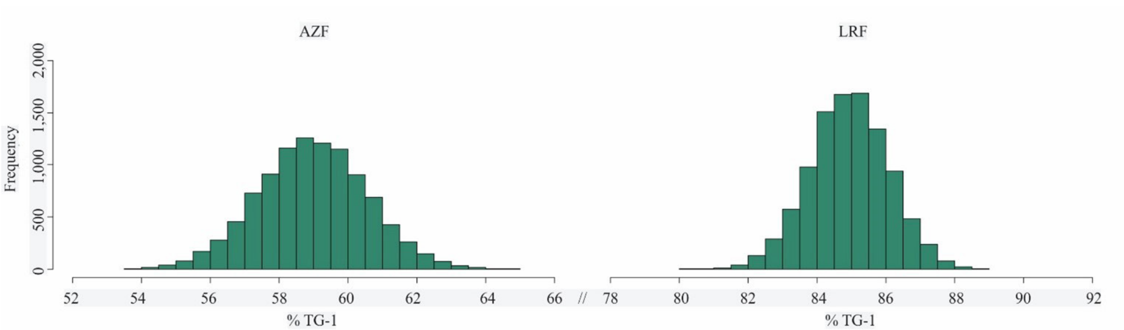

FIG. S1. Histogram. Frecuency distribution in which whole spinicaudatans (TG-1) are obtained by performing statistic for the Triassic paleolakes of the Agua de la Zorra (**AZF**) and Los Rastros (**LRF**) formations. %= percentage.

2. Chi-square test

The chi-square test is used to evaluate the independence between variables in my samples of different sizes (Pearson, 1900). The analysis was performed using the number of spinicaudatans collected complete (TG-1) and fragmented (TG-2) in LRF and AZF. Data are available in the supplementary materials (Table S1).

Pearson's chi-square test with Yates' continuity correction yielded an *X-squared*=258.58, with a degree of freedom (*df*)=1, for a *p-value* <2.2e-16. This statistical test yielded the following data table (Table S4). The results obtained from this test indicate that the TGs recorded for LRF are significantly different from the TGs recorded for AZF.

TABLE S4. DATA TABLE OF THE CHI-SQUARE RESULTS FOR THE SAMPLES ANALYZED FROM LOS RASTROS FORMATION (LRF) AND AGUA DE LA ZORRA FORMATION (AZF).

Measurements	Min.	1st Qu.	Median	Mean	3rd Qu.	Max.
LRF	429.2	589.6	750	750	910.4	1070.8
AZF	471.8	648.2	824.5	824.52	1000.8	1177.2

3. Conclusion of the statistical analysis

Both statistics used are consistent in their results. The resampling and Pearson's chi-square test affirm that the percentages of spinicaudata shell preservations significantly differ between the AZF and LRF paleolakes.

References

Pearson, K. 1900. On the criterion that a given system of deviations from the probable in the case of a correlated system of variables is such that it can be reasonably supposed to have arisen from random sampling. Philosophical Magazine 50: 157-172.